





SYSTEMATICS AND PHYLOGENY

Biogeography and integrative taxonomy of *Epipterygium* (Mniaceae, Bryophyta)

Maximilian Hanusch,^{1,2}  Edgardo M. Ortiz,¹  Jairo Patiño^{3,4*}  & Hanno Schaefer^{1*} 

¹ Department Ecology & Ecosystem Management, Plant Biodiversity Research, Technical University of Munich, Emil-Ramann Str. 2, 85354 Freising, Germany

² Department of Biosciences, Functional Community Ecology Research Group, University of Salzburg, Hellbrunnerstr. 34, 5020 Salzburg, Austria

³ Departamento de Botánica, Ecología y Fisiología Vegetal, Universidad de La Laguna, La Laguna, Tenerife, Spain

⁴ Island Ecology and Evolution Research Group, Instituto de Productos Naturales & Agrobiología (IPNA-CSIC), La Laguna, Tenerife, Spain

* Contributed equally

Addresses for correspondence: Hanno Schaefer, hanno.schaefer@tum.de; Jairo Patiño, jpatino@ull.edu.es

DOI <https://doi.org/10.1002/tax.12324>

Abstract A significant number of bryophyte species are thought to have transcontinental geographic ranges, often with multiple disjunct distribution areas. One of these cases is *Epipterygium tozeri* (Mniaceae), with a Holarctic distribution and disjunct ranges in western North America, the Mediterranean, Japan and central Asia. Collections from different geographic regions were lumped into *E. tozeri* based on morphology, but a molecular confirmation was lacking so far. Here, we tested species concepts in the genus *Epipterygium*, with a special focus on the *E. tozeri* species complex, combining morphological and DNA sequence data for the nuclear ribosomal ITS region and two plastid loci (*trnG* intron, *trnT-psbD* spacer). In a second step, we reconstructed the historical biogeography of the genus. We found that *Epipterygium* most likely originated in Asia or North/Central America and that the alleged single widespread species *E. tozeri* with disjunct ranges is in fact a group of genetically and morphologically distinct taxa, including four overlooked species, for which we provide descriptions: *E. atlanticum* sp. nov., *E. bauritum* sp. nov., *E. oreophilum* sp. nov., and *E. yunnanense* sp. nov. The biogeographical history of these species is best explained by a step-wise parallel colonization of the Eurasian and American continents followed by *in-situ* speciation.

Keywords Bryophytes; cryptic species; disjunctions; Macaronesia; Mediterranean

Supporting Information may be found online in the Supporting Information section at the end of the article.

■ INTRODUCTION

Species delimitation is one of the central issues in Systematics, especially in groups with reduced morphology like bryophytes, which have a limited number of diagnostic characters. Although DNA-based methods have in some cases resulted in lumping bryophyte species with broad distributions (Vanderpoorten & Shaw, 2014), integrative taxonomic approaches have also resulted in the discovery of previously overlooked species that exhibit narrower distribution ranges (e.g., Renner & al., 2010; Sukkharak & al., 2011; Medina & al., 2012). Species-rich and morphologically not very distinct bryophyte families, such as the Bryaceae and Mniaceae, are particularly hard to revise based on morphological data alone (Holyoak & Pedersen, 2007). In consequence, the generic circumscriptions in these two families changed considerably when DNA data and molecular phylogenetic analyses became available (Cox & Hedderson, 1999; Pedersen & al., 2003; Newton & al., 2006).

Among the numerous affected genera is *Epipterygium* Lindb. (Mniaceae), which was described in 1862 to accommodate the two species *E. wrightii* (Sull.) Lindb. and *E. jamaicense* Lindb. (Lindberg, 1862). Today, there are 17 validly described names listed for *Epipterygium* (see <http://www.theplantlist.org>). Three of them have been transferred to other genera: *E. limbatulum* (Renauld & Cardot) Besch. and *E. pacificum* Besch. are in the genus *Eriopus* Brid. (Paris, 1900; Fleischer, 1922), and *E. diversifolium* Renauld & Paris has been transferred to *Bryum* (Bizot, 1971). *Epipterygium lepidopiloides* (Müll.Hal.) Paris has been synonymized with *E. immarginatum* Mitt. (Shaw, 1984), and *E. obovatum* Ochya has been synonymized with *E. opararensis* Fife & A.J.Shaw (Fife & Knightbridge, 2005). The remaining 12 currently accepted species were mostly described in the late 19th or early 20th century (Lindberg, 1862; Mitten, 1871; Brotherus, 1892; Dusén, 1895; C. Müller, 1897b, 1901) or moved to the genus during the same period (Lindberg, 1864; Paris, 1900; Brotherus, 1909). In the second half of the 20th century, three less common

Article history: Received: 14 Oct 2019 | returned for (first) revision: 21 Feb 2020 | (last) revision received: 15 Jun 2020 | accepted: 23 Jun 2020

Associate Editor: Alain Vanderpoorten | © 2020 The Authors.

TAXON published by John Wiley & Sons Ltd on behalf of International Association for Plant Taxonomy.

This is an open access article under the terms of the Creative Commons Attribution-NonCommercial-NoDerivs License, which permits use and distribution in any medium, provided the original work is properly cited, the use is non-commercial and no modifications or adaptations are made.

species, *E. koelzii* H. Rob., *E. opararensis* and *E. vanuatuicum* H. A. Mill. have been described, the two latter only occurring as local endemics on islands (Robinson, 1968; Miller, 1988; Fife & Shaw, 1990). However, several species received little or no taxonomic attention since their publication and might only represent regional varieties (Crum, 1967; Fife & Shaw, 1990).

Most of the 12 accepted *Epipterygium* species have a tropical distribution. The only species extending into temperate regions is Tozer's Thread-Moss, *E. tozeri* (Grev.) Lindb. It is also thought to be the only *Epipterygium* species with an intercontinentally disjunct range, including populations in western North America, Europe, central Asia, Japan and Taiwan (Crundwell & al., 1982; Arts & Nordhorn-Richter, 1986; Shaw, 2001). *Epipterygium tozeri* was described in the early 19th century as *Bryum tozeri* Grev. (Greville, 1827). Since then, only regional revisions of the genus have been published (Crum, 1967; Shaw, 1984; Ochi, 1985), lacking a wide geographic or taxonomic scope that could contribute to a better understanding of the evolution and historical biogeography of the species complex.

The pattern of disjunction between the Pacific coast of North America and the Mediterranean region of southern Europe, also known as Madrean-Tethyan disjunction (Axelrod, 1958, 1975), is found in several vascular (Wen & Ickert-Bond, 2009) but mainly in non-vascular plants (e.g., Heinrichs & al., 2009; Patiño & Vanderpoorten, 2018). It has been explained by vicariance driven by continental drift, which caused the fragmentation of ancestral distribution ranges at the end of the Oligocene (Axelrod, 1975). In this context, a transcontinental distribution of *E. tozeri* along the southern shoreline of the Laurasian continent before continental breakup has been suggested (Arts & Nordhorn-Richter, 1986). However, for many vascular plant taxa with similar distribution patterns such as the one exhibited by the *E. tozeri* complex, it has been suggested that their current distribution is the result of overland migration by a common ancestor. The western North American–western Eurasian disjunction has thus been explained by a number of alternative hypotheses: (i) to be the result of a long-distance dispersal (LDD) event followed by later parallel adaptation to local conditions in Europe and North America (Meusel, 1969; Axelrod, 1975; reviewed in Kadereit & Baldwin, 2012); (ii) to have emerged from dispersal across the Bering Land Bridge since the Tertiary around 66 Ma (Tiffney & Manchester, 2001) and before the Bridge sundered around 5.5 Ma; or (iii) to have been promoted by dispersal across the North Atlantic Land Bridge between 30 and 40 Ma (Tiffney, 2000), followed by extinction in eastern and persistence in western North America (reviewed in Milne & Abbott, 2002; Milne, 2006).

While support for the Madrean-Tethyan hypothesis could be found for several seed plant genera (e.g., Fritsch, 2001; Hileman & al., 2001) and a few bryophyte lineages (e.g., Patiño & al., 2017), most bryophyte studies to date have shown that intercontinental disjunction is better explained by recent LDD events rather than vicariance (Werner & al., 2003; Shaw & al., 2003; Huttunen & al., 2008). However, whereas the North

Atlantic Land Bridge has received null support from genetic evidence in bryophytes (Désamoré & al., 2016), a number of studies have provided support (Shaw & al., 2014; Kyrkjõeide & al., 2016) or rejected the Beringian Land Bridge hypothesis (Patiño & al., 2016), leaving the biogeographic mechanisms driving the western North American–western Eurasian disjunction poorly understood. Some studies revealed low or no molecular and morphological variation among the disjunct bryophyte populations in western North America and Europe (e.g., Werner & al., 2005; Davison & al., 2006; Vigalondo & al., 2016, 2019b), while other studies discovered previously overlooked species (Medina & al., 2012, 2013; Caparrós & al., 2016), including examples of extreme LDD events followed by speciation (e.g., Patiño & al., 2013; Vigalondo & al., 2019a). Hence, there is apparently no uniform pattern, and each case of supposed disjunct distribution needs to be analyzed independently.

The general aim of the present study was to perform a comprehensive molecular and morphological analysis to infer phylogenetic relationships and reconstruct the biogeographic history of the genus *Epipterygium*, with a special focus on the *E. tozeri* species complex. In this framework, our specific goal is to identify the best-fitting species hypothesis for the *E. tozeri* complex. Based on preliminary morphological evidence from literature (Shaw, 1984), we hypothesized that the widely disjunct populations of *E. tozeri* represent distinct taxonomic entities. With the combination of disjunct populations, morphological ambiguity and a complex taxonomic history, the genus *Epipterygium* in general and the *E. tozeri* species complex in particular seemed an optimal choice to test the strength of such an integrative taxonomic approach.

■ MATERIAL AND METHODS

Material. — Thirteen collections of Macaronesian *E. tozeri* were made in the Canary Islands in Nov./Dec. 2017 on the islands of El Hierro, La Palma, Tenerife and Gran Canaria (Collection permit numbers: El Hierro: NRE 12338; Gran Canaria: O00006501_17_0016341; La Palma: A/EST-022/2017; Tenerife: AFF 311/17). In addition, 173 herbarium specimens of seven *Epipterygium* species were obtained from the herbaria BSM, DR, E, LG, LISU, M, MO, NY, S, TUM and the private collection of A. Schäfer-Verwimp (Herdwangen-Schönach, Germany). We lacked material for five species: *E. brasiliense* E. B. Bartram from Brazil, *E. koelzii* H. Rob. from India, *E. mandonii* (Müll. Hal.) Paris from Bolivia, *E. rigidum* Lindb. from the Caucasus, and *E. vanuatuicum* H. A. Mill. from Vanuatu. Most of these five species are known only from the type locality and were described based on few diagnostic morphological characters or without a comprehensive understanding of the genus (Brotherus, 1892; C. Müller, 1897a,b; Bartram, 1952; Robinson, 1968; Miller, 1988). For example, both *E. rigidum* and *E. vanuatuicum* are known only from old type material impeding their inclusion in a molecular phylogenetic study. During visual inspection of the

specimens from the West Indian Islands it turned out that four collections match well the description of *E. orbifolium* Müll. Hal. (C. Müller, 1879) rather than *E. wrightii*. In a previous study, Shaw (1984) did not perform a formal synonymization of the two taxa and we therefore refrain from doing it here and list the mentioned specimens as *E. orbifolium*. A total of 186 *Epipterygium* specimens were examined in the study, including 142 specimens of *E. tozeri* that were sampled from its entire worldwide range except Taiwan. Two sequences of the sister genus *Pohlia* were downloaded from GenBank as outgroup.

Morphological analyses. — To explore the possible existence of phylogenetic patterns evidenced by morphological variation within the *E. tozeri* group, one or two collections of each main clade identified in the phylogenetic analysis (see Results) were randomly selected. Five gametophytes per collection were randomly chosen and measured, adding up to a total of 55 gametophytes (details about the specimens studied are provided in Appendix 1). For the distinct lineage from Yunnan Province, only one collection (*D.G. Long s.n.*, E barcode E00576940) could be analyzed, whereas for the Iranian sample (*H. Zarre Bl. 73486*), the plant tissue was too limited for morphological analyses.

Ten continuous characters and four ratios derived from these measurements (Appendix 1) were used for the morphometric analyses, following the approach proposed by Shaw (1984). Upper non-perichaetial leaves were chosen to measure cell length and width, including the cell wall, each from the same cell. Ventral and dorsal leaf sizes, along with ventral leaf costa lengths, were measured on the same leaves. We first performed a principal component analysis (PCA) to explore for unknown underlying structure in our dataset. To minimize variance inflation, we excluded all characters that were strongly correlated to another character using the R package *usdm* v.1.1-18 (Naimi & al., 2014). To detect the collinearity among the variables, we calculated the variance inflation factor (VIF) and excluded all variables with a VIF > 10. Excluded variables were median cell length, lateral leaf length and marginal cell width. With this pruned dataset, a discriminant function analysis (DFA) was performed to test the statistical support of the predefined geographical groups, allowing us to continue with descriptive statistics using the geographic regions as a grouping variable. Univariate variance analysis (ANOVA) and post-hoc analysis with Tukey-Test were conducted on the variables to compare homogeneity of variances and infer the level of variation between the geographic groups. All these statistical analyses were performed in R v.3.6.1 (R Core Team, 2019).

DNA extraction and sequencing. — Ten gametophytes per collection were placed in the -80°C freezer for 20 min and then ground in a mixer mill (MM 400, Retsch Laborgeräte, Haan, Germany), with three stainless steel beads per tube. The samples were ground for 2 min, then re-frozen and ground again for 2 min. DNA extraction was carried out with the NucleoSpin Plant DNA Extraction Kit (Macherey-Nagel, Düren, Germany) following the manufacturer's protocol.

Total genomic DNA yield was evaluated using an EPOCH Microplate Spectrophotometer (BioTek, Winooski, Vermont, U.S.A.). One nuclear and two chloroplast regions were amplified. The nuclear internal transcribed spacer (ITS) 1 and 2 regions, including the 5.8S ribosomal RNA gene, were amplified using the primers ITS-Br5 (CCTTATCATTTAGAG GAAGGAG) and ITS-Br4 (CCGCTTAKTGATATGCTTAA) designed by Cheng & al. (2016). When PCR amplification with these primers failed, internal primers ITS-Br2 (GCCAAGATATCCGTTGCTGAG) and ITS-Br3 (YRACT CTCAGCAACGGATA) designed by Cheng & al. (2016) were used. The chloroplast *trnT-psbD* intergenic spacer was amplified with primer pair *psbD-PT* (GGGACCAGTCATC CATACTATC) and *trnT-PT* (AAGGCGTAAGTCATCGG TTC) (Nishiyama & Kato, 1999), and the *trnG*-intron with the primer pair *trnGF* (ACCCGCATCGTTAGCTTG) and *trnGR* (GCGGGTATAGTTT TAGTGG) developed by Pacak & Szweykowska-Kulińska (2000). Amplification was carried out with KAPA 2G Fast HotStart ReadyMix (Kapa Biosystems, Wilmington, Massachusetts, U.S.A.). The polymerase chain reaction (PCR) was performed with 1 μl of template DNA, 7.5 μl of KAPA 2G Fast HotStart ReadyMix and 0.75 μl of 10 pM upstream and downstream primer. The PCR mix was then filled up with 5 μl of double-distilled H_2O to a total of 15 μl . If the first PCR did not yield any product, a second PCR was conducted with either half or double the amount of template DNA. In that case, the amount of H_2O was adjusted to fit the total volume of 15 μl . Thermal cycler settings were optimized by lowering the annealing temperature to 50°C . The PCR included one cycle of denaturation at 95°C for 180 s, 35 cycles of 15 s denaturation at 95°C , 15 s of annealing at 50°C , 15 s of extension at 75°C , followed by a final extension of 90 s at 75°C . The PCR products were checked for the presence of single bands of the expected size on a 1% agarose, stained with Roti-GelStain (Carl Roth, Karlsruhe, Germany). Purification of the PCR-products was done with Exo-Sap (Fermentas, St. Leon-Rot, Germany), consisting of 1 μl shrimp alkaline phosphatase and 0.25 μl of exonuclease 1. Sequencing was carried out by GATC Biotech (Konstanz, Germany) using Sanger ABI 3730xl technology. Forward and reverse sequences were edited, assembled and aligned in Geneious v.11.0.5 (Biomatters, Auckland, New Zealand), using the implemented MAFFT-alignment algorithm. Alignments were visually examined in PhyDE-1 v.0.9971 (Phylogenetic Data Editor, J. Müller & al., 2005). Finally, 168 ambiguous positions were excluded, and indels were coded as binary characters ($n = 339$, see suppl. Appendix S1 and S2) using SeqState v.1.4.1 (K. Müller, 2005), following the simple indel coding method of Simmons & Ochoterena (2000).

Phylogenetic analyses. — Phylogenies were inferred using maximum-likelihood (ML) and Bayesian approaches on an alignment of 109 specimens which yielded sufficient DNA to be successfully sequenced (Appendix 2). Bayesian tree inference was performed with MrBayes v.3.4.6 (Huelsenbeck & Ronquist, 2001), and ML analysis was done in IQ-TREE v.1.6.10 (Nguyen & al., 2015). Best-fitting DNA substitution

models, as well as rate of invariable sites and gamma rates, were selected for each gene locus separately with Partition-Finder 2 (Lanfear & al., 2017) based on the corrected Akaike information criterion (Akaike, 1974). Best-fitting models were HKY+ Γ for ITS, GTR+ Γ for *trnT-psbD* and HKY+ Γ for *trnG*. For the coded indels, we selected the GTR2+ASC model, which is recommended for binary data (Ronquist & al., 2011; Minh & al., 2019). First, we analyzed chloroplast and nuclear DNA regions separately and compared all well-supported clades in the ITS ML tree and the chloroplast ML tree to detect possible significant conflicts in topology. Since no well-supported (>75% bootstrap [BS]) topological conflicts could be detected, we concatenated all DNA regions and the coded indels. With that dataset, an ML-tree with 5000 ultrafast-bootstrap replicates was calculated, and the ultrafast bootstrap (UFBS) (Hoang & al., 2018) results were uploaded to the RogueNaRok webpage (<https://rnr.h-its.org/>, Aberer & al., 2013) to screen the tree for any ambiguously placed specimens, which should be excluded from the dataset. Since all specimens were unambiguously placed, we continued the tree inference with the full alignment.

For ML-tree estimation, we ran four parallel searches with 250 standard BS replicates, each for a total of 1000 BS replicates. We further performed one additional ML search with UFBS values (Hoang & al., 2018) derived from 5000 replicates. To minimize the risk of tree search being stuck in local optima, tree inference was performed with an increased stopping iteration of 150. The resulting five ML trees showed no conflicts in topology, so the one with the highest likelihood was chosen for display.

Bayesian tree inference was then performed with four MrBayes runs of 20 million generations each, with tree sampling every 1000 generations. Convergence was checked by visualizing the log files in Tracer v.1.7 (Rambaut & al., 2018) and checking that all parameters reached stationarity and effective sampling sizes >200. A 50% majority-rule consensus tree with posterior probabilities (PP) was calculated after discarding a burn-in of 25% with sumtrees.py v.4.4.0 (Sukumaran & Holder, 2010). We then used sumtrees.py to plot PP values from the Bayesian analysis on our ML target tree, and then used IQ-TREE to add the support values from the standard 1000 BS and the 5000 UFBS, so every node was annotated with three alternative support values. The ML tree was plotted using FigTree v.1.4.3 (Rambaut, 2016).

Molecular dating and ancestral area reconstructions.

— A molecular dating analysis was performed on a reduced combined dataset of 107 specimens of seven species excluding the coded indels (suppl. Appendix S3). One specimen of *E. mexicanum* for which we had obtained only one chloroplast DNA region was removed. We further screened the dataset for identical sequences in order to perform the analysis on the haplotype level and excluded one sequence of *E. tozeri*. To prune identical sequences, we used the R-package seqinr v.3.4 (Charif & Lobry, 2007). Ultrametric trees were inferred with BEAST v.1.10 (Suchard & al., 2018) using a strict clock and an uncorrelated lognormal relaxed clock model. For each

of the clock model priors, we used two different absolute nucleotide substitution rates in one single run: (i) the substitution rate for the two chloroplast regions was set to $4.453e-4 \pm 1.773e-6$ substitutions/site/million years following Patiño & al. (2017); and (ii) the substitution rate for the nuclear ITS region was set to 0.00135 ± 0.005 substitutions/site/million years with a normal prior distribution and truncated with upper and lower bounds of $0.4e-3$ and $8.3e-3$ substitutions/site/million years (Bechteler & al., 2017). Three different models, including a Yule model, a birth-death model, and a coalescent model with constant population sizes were compared for performance, each under a strict and a relaxed clock. Model comparison was achieved by a Bayes factors analysis. First, marginal likelihood estimates (MLEs) were calculated through a stepping-stone and a path sampling method, respectively, with 100 steps with priors set as in Patiño & al. (2017). Resulting MLEs for the different combinations of parameters were ranked, and Bayes factors were calculated as two times the difference between the best-fitting and alternative models ($2\ln Bf$). Bayes factor analysis gave the birth-death model under a relaxed clock as best-fitting model (Appendix 3). The model was run for 100 million generations on four independent runs, with sampling every 10,000 generations. Log files were checked for convergence and good mixing in Tracer v.1.7 (Rambaut & al., 2018) after discarding a burn-in of 25%. A maximum clade credibility tree was calculated from the remaining 30,000 trees.

The maximum clade credibility tree was used to perform an ancestral area estimation analysis after removing the outgroups. Distribution data of specimens was compiled from herbarium labels, and each haplotype was assigned to one or several of the eight geographic regions considered: Macaronesia (A), Europe (B), Middle East (C), Asia (D), Africa (E), South America (F), Central America/Caribbean (G), and North America (H). We performed ancestral area estimations with the R package BioGeoBEARS v1.1.1 (Matzke, 2014). In BioGeoBEARS, the Lagrange DEC model (dispersal-extinction-cladogenesis) can be implemented, which includes dispersal (d) and extinction (e) as free parameters, and a model (DEC+J) that includes an additional parameter J that takes founder-event speciation into account (see Matzke, 2014). Since different approaches to estimate ancestral areas are based on different assumptions, one can compare these two versions of the DEC model with a likelihood version of the dispersal-vicariance analysis (DIVALIKE), and a likelihood version of the range evolution model of the Bayesian binary model (BAYAREALIKE), with the option of also adding founder-event speciation to either of them. However, in a recent study, Ree & Sanmartín (2018) concluded that DEC+J might be a poor model for founder-event speciation, and statistical comparisons of its likelihood with a pure DEC model may be inappropriate. Consequently, we refrained from implementing DEC+J in the present study and focused on the classical versions of the three biogeographical models implemented in BioGeoBEARS (DEC, DIVALIKE, BAYAREALIKE). These three models were estimated in a maximum likelihood

framework and compared in terms of how well they fitted the data using the Akaike information criterion corrected for small sample size (Matzke, 2013, 2014), which resulted in DIVA-LIKE as best-fitting model for our dataset (Appendix 4).

Molecular species delimitation. — A Bayesian implementation of the general mixed Yule-coalescent model (bGMYC) provided in the R-package *bgmyc* v.1.0.2 (Reid & Carstens, 2012) and a multi-rate Poisson tree process (mPTP) provided at the mPTP webpage (<https://mptp.h-its.org>) (Kapli & al., 2017) were used to obtain preliminary species hypotheses. The PTP model (Zhang & al., 2013) and the GMYC-Model (Pons & al., 2006) are likelihood-based attempts to assign branches in a gene tree as either intra- or interspecific. The Bayesian implementation of the GMYC model reduces the potential error in phylogeny estimation and the uncertainty in model parameters and uses a set of ultrametric trees as input. The multi-rate implementation of the PTP model allows every putative species to evolve with different evolutionary rates and uses a single ML tree as input. To run the mPTP model on our dataset, we uploaded the previously estimated ML tree. As recommended by Monaghan & al. (2009) and Patiño & al. (2017), 100 trees from the BEAST output were randomly sampled after a 25% burn-in, and the bGMYC analysis was performed with 50,000 generations per sample, discarding the first 40,000 generations as burn-in and using a thinning factor of 100. The outgroup was removed before running the analyses, and the results of both species delineation methods were then discussed as possible taxonomic hypotheses. Additionally, we set up an alternative hypothesis for the taxonomic treatment (H1) that integrates delineation concepts of both models, geographic origin and the results of our morphological character investigation, while avoiding a taxonomical overpartition of the *E. tozeri* species complex. In this treatment, the clades from Macaronesia, continental Europe, North America, and Asia were treated as distinct taxa based on the integration of morphological, molecular and distribution attributes. The specimens from Iran and Yunnan were addressed as singletons due to their molecular and geographic uniqueness. The remaining species in the genus were treated likewise, resulting in a total of six additional entities.

Molecular species validation. — Three different species delimitation schemes were tested with a Bayes factor analysis, following the framework of Grummer & al. (2014). This approach compares alternative groupings obtained by lumping and splitting different lineages in competing models generating a marginal likelihood estimate of a species tree for each model. MLEs were assessed using the path sampling method (Lartillot & Philippe, 2006), with 100 path steps, a chain length of 100,000 generations and likelihoods saved every 2000 generations, following the framework of Patiño & al. (2017). Species trees for different hypotheses were inferred using StarBEAST2 v.2.5 (Ogilvie & al., 2017). A uniform prior was set for the strict clock with an initial value of 1.0 and an upper bound of 25. A Yule process with a linear and constant root population-size model was chosen for

species tree estimation. For the population mean prior, an inverse gamma distribution with an initial value of 0.02, shape set at 3.0 and scale set at 0.3 was selected. For the Yule process birth rate, an inverse gamma distribution with an initial value of 1.0, shape set at 0.5 and scale set at 1.0 was chosen.

■ RESULTS

Morphometric analyses. — The morphometric analysis consisted of 550 individual measurements of gametophyte traits and 220 ratios derived from the variables across 11 collections of *E. tozeri* (Appendix 1). Quantitative characters and the ratios indicate a high level of variation among the populations from different geographic regions (Fig. 1). The results of the PCA showed that the first two principal components (PCs) accounted for 45.2% of the variance. The American and continental European specimens were placed in distinct clusters, with only a small overlap to the Japanese sub-region. Specimens from Yunnan showed a high degree of overlap with Macaronesian and Japanese samples. Asian samples were distinct from all other clusters. The most important variable in PC1 was related to costa length (24.87% overall contribution). Continental European, northern American and Japanese samples show larger values for these variables. According to PC2, the most important variable was marginal cell width (24.75% overall contribution; also see suppl. Fig. S1). Continental European and Macaronesian samples have significantly larger values for this variable (see Appendix 1). After excluding the highly correlated variables from our dataset, the DFA classified all the cross-validated group samples correctly to the clades identified from the phylogenetic tree inference (see below). All 14 variables show statistically significant differences between the five sub-groupings (Appendix 1). *Epipterygium tozeri* samples from continental Europe have the longest median cells, whereas specimens from northern America show the highest lateral leaf length/width ratio and can be easily distinguished by a second row of dorsal leaves. Asian and Macaronesian specimens have significantly shorter stems than all other specimens, while Macaronesian specimens show much longer median cells than the Asian samples. The Asian specimens have the shortest lateral leaves of all populations. Specimens from the population of Yunnan are characterized by short dorsal leaves and can be differentiated from Macaronesian populations by stem length. Japanese *Epipterygium* specimens have the shortest marginal cells together with the Asian samples but can be differentiated from those by their longer stems. Specimens from North American, Japanese, Asian and Yunnan populations all have more or less strongly developed serration at their perichaetial leaf apices, whereas specimens from Macaronesia and continental Europe show entire perichaetial leaf margins. To confirm the results of the quantitative morphological analysis as well as the distinctive features (e.g., serration of perichaetial leaves), all specimens listed in Appendix 2 were subsequently examined visually and confirmed for these characteristics.

Sequences and alignment. — In total, we produced 289 sequences for 109 specimens of seven *Epipterygium* species. Seventy-six of the initial 142 samples of *E. tozeri* could be included in the molecular analyses: 62 from Europe, 7 from Asia, 6 from North America and 1 from the Middle East. Unfortunately, we did not manage to obtain any usable sequences of the Japanese *E. tozeri* samples and specimens of *E. opararens* from New Zealand. The concatenated alignment length was 2294 nucleotides plus an additional 339 binary characters from the indel coding, summing up to a total length of 2633 sites (Table 1).

Phylogenetic inference. — Maximum likelihood and Bayesian tree estimation returned highly consistent results (Fig. 2). Ten major clades were highly supported and congruent in both cases. All samples were placed in two major clades,

one clade consisting of all the Afro-Eurasian specimens, and a second clade comprising all specimens from northern and southern America. The *E. tozeri* samples are not monophyletic but rather cluster by geographic origin. The North American *E. tozeri* samples are sister to all other *Epipterygium* species from the Americas. The European samples are placed in two major polytomies: one includes mostly samples of continental-mediterranean origin, the other mainly specimens from the Macaronesian islands. One specimen from Scotland was nested within the Macaronesian clade, whereas one specimen from Madeira grouped in the continental-mediterranean clade. The Asian samples were placed in two different clades: one comprises specimens from the western part of China and Iran, the other is sister to the African species and includes the specimens of Himalayan origin. All Eurasian specimens

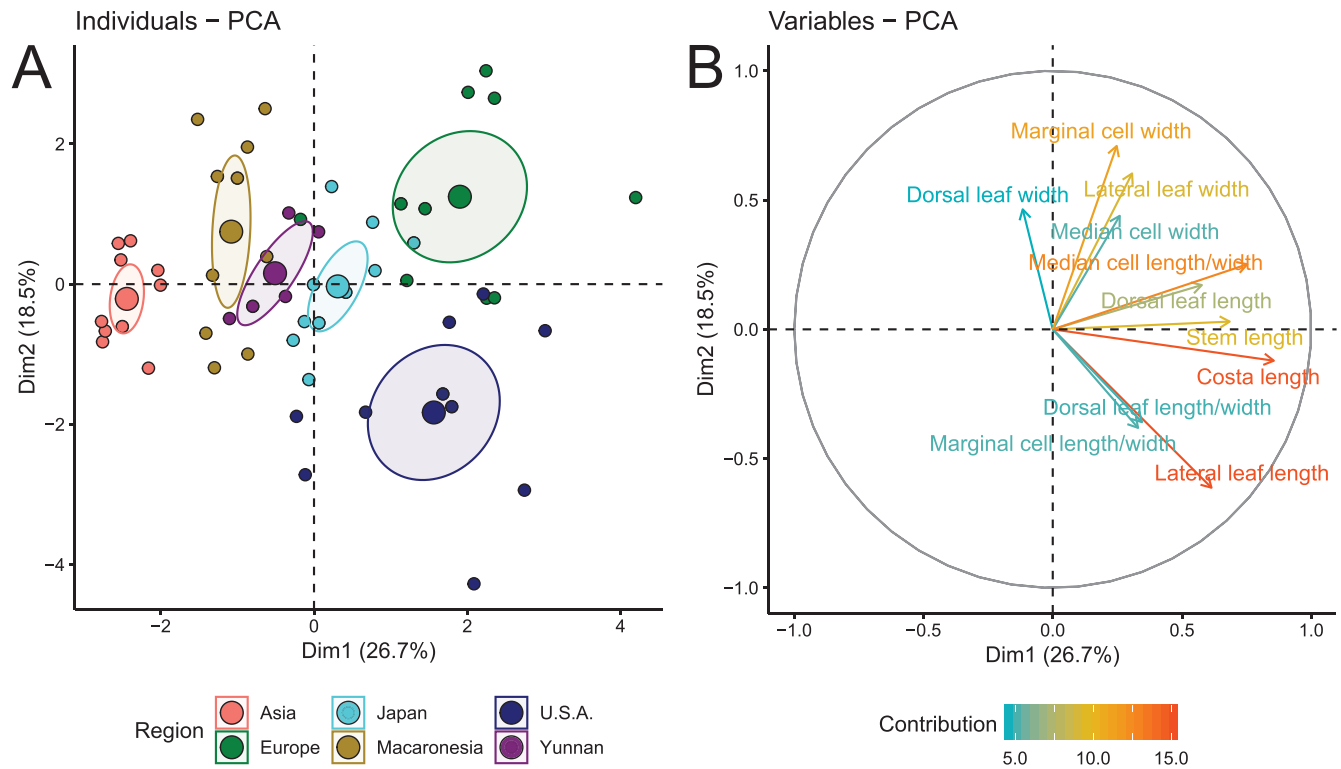


Fig. 1. **A**, Results of the principal component analysis (PCA) for *Epipterygium tozeri* specimens. Colors represent the six different populations of *E. tozeri* s.l. Individual specimens are shown by small points, big points represent group means, and 95% confidence ellipses were drawn around group means; **B**, The correlation of each measured trait to the PCA is displayed by vectors. Coloration and arrow length represent contribution to total variance.

Table 1. Number of sequences, sequence length, unique sites, informative characters and invariant sites for the analysed DNA regions.

Region	Type	Sequences	Sites	Unique sites	Informative characters	Invariant sites
ITS1+2	nuc DNA	103	1054	155	176	722
<i>trnT-psbD</i>	cp DNA	99	617	22	56	539
<i>trnG</i>	cp DNA	104	623	38	29	556
Indels	binary	110	339	165	174	0

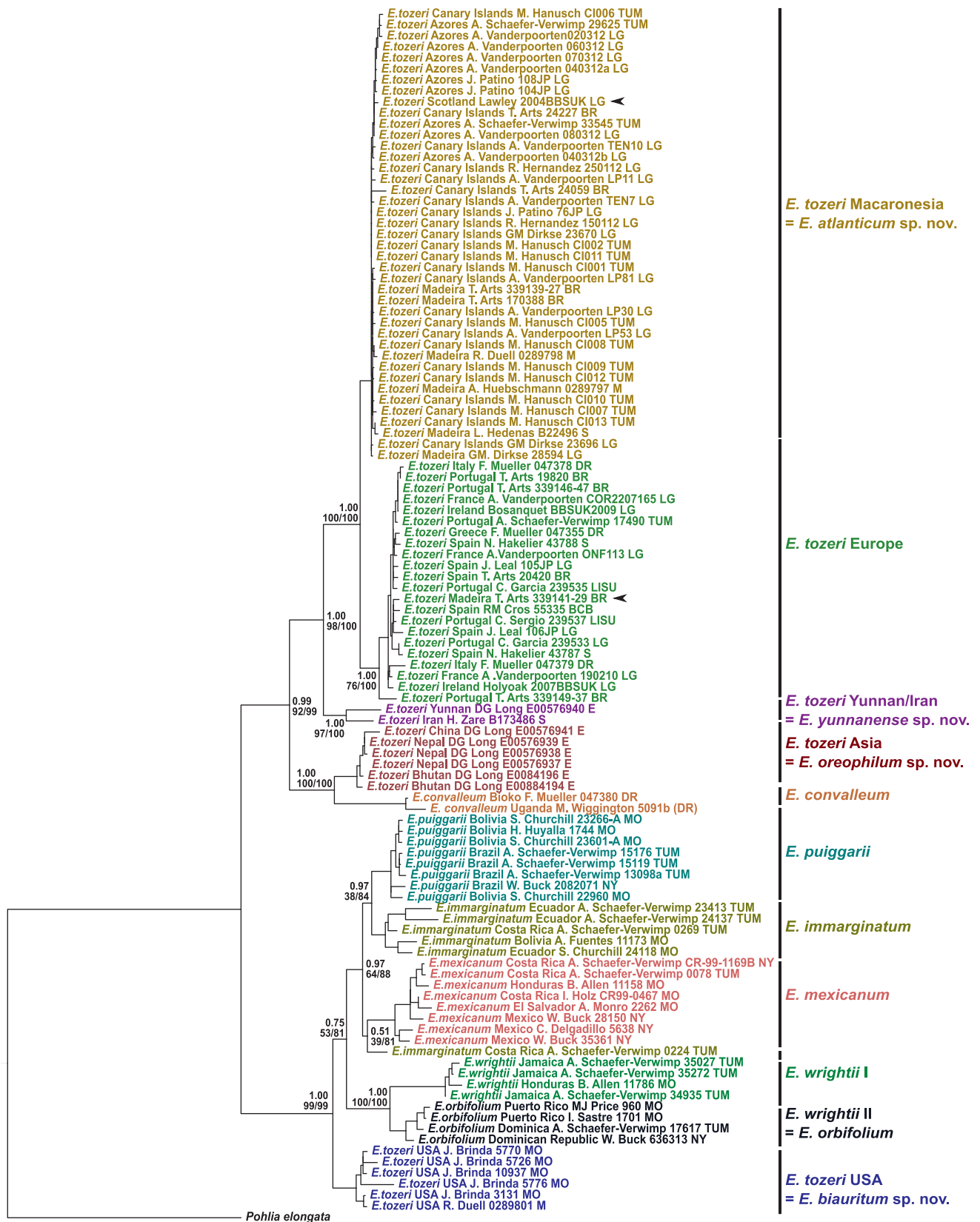


Fig. 2. Single best ML tree for 109 *Epipterygium* specimens inferred from the partitioned ITS + chloroplast DNA matrix plus coded indels. Regular bootstrap and ultrafast bootstrap values are shown on the branches, posterior probabilities above the bootstrap values. Black arrows indicate the *E. tozeri* specimen from Scotland that was nested within the Macaronesian clade and one specimen from Madeira that grouped in the Mediterranean-Continental clade.

of *E. tozeri* are paraphyletic with respect to the two African specimens of *E. convalleum*. Except for one specimen of *E. immarginatum* that did not group with the other specimens of this taxon, all species from the New World form monophyletic groups.

Molecular dating and biogeography. — The chronogram resulting from the BEAST analyses of the concatenated nuclear and chloroplast regions was highly congruent with the ML and MrBayes phylogenies. The split between the New World and the Old World clades was inferred at 58.8 Ma with a highest posterior density (HPD) of 31.5–89.7 Ma (Fig. 3). The continental Europe-Macaronesia disjunction was estimated at 10.3 Ma (HPD 4.9–17 Ma), whereas the Himalayas-African disjunction was dated back to ca. 17.3 Ma (HPD 5.6–31.2 Ma). The diversification of the Neotropical species set in 23.5 Ma (HPD 13.4–36 Ma).

The results of the biogeographic range analysis indicate that the genus *Epipterygium* most probably originated in Asia, North or Central America (Fig. 3). Our inference of ancestral areas suggests that the European continent and Macaronesia were colonized from Asia about 11–37 Ma, while the African continent was probably reached from Asia by a single LDD event. The diversification within America involved a potential split between adjacent areas across Central and North America 16–47 Ma. The radiation of the Caribbean species *E. wrightii* and *E. orbifolium* started 4–17 Ma, while the Central American species *E. mexicanum* and the mainly South American species *E. immarginatum* and *E. puiggarii* started radiating ca. 6–16 Ma. The colonization of South America by a Central American ancestor involved a single LDD event, with the split between South American and Central American lineages estimated ca. 8–23 Ma. We also inferred a possible event of reverse colonization from South to Central America in *E. immarginatum*.

Molecular species delimitation. — We identified 11 molecular entities running the mPTP model, whereas the bGMYC model delineated 14 molecular entities, some of them consisting of only one haplotype. Both models congruently delineated *E. orbifolium*, *E. wrightii*, *E. convalleum* and the specimens from the Himalayas as molecular entities (Fig. 3) Under the mPTP model, specimens from Iran and western China grouped together as one entity, whereas specimens of *E. tozeri* from Macaronesia and continental-mediterranean Europe were delineated as two distinct species with an additional pair within the mainly Macaronesian clade and a singleton in the mainly continental clade. The mPTP model grouped all southern American specimens of *E. immarginatum*, *E. mexicanum* and *E. puiggarii* together, whereas the bGMYC model delineated three molecular entities that are nested within the *E. immarginatum* cluster. Additionally, the bGMYC approach split *E. tozeri* specimens from Iran and western China and delineated two clades within the North American *E. tozeri* cluster.

Our taxonomical hypothesis H1, which is a synthesis of geographic origin, morphological variation and molecular species delineation approaches, received the highest support

by the path sampling method. Bayes factors distinguished this hypothesis clearly from the mPTP model (2lnBF = 58.12) and the model provided by bGMYC analysis (2lnBF = 30.46).

■ DISCUSSION

Our phylogenetic analyses and morphological measurements revealed a considerable geographic structure within the *Epipterygium tozeri* complex. Recent studies often showed low or no morphological and phylogenetic differentiation between populations of intercontinentally disjunct bryophytes (e.g., Shaw & al., 2003; Heinrichs & al., 2009; Kreier & al., 2010; Lewis & al., 2014; Patiño & al., 2016; Vigalondo & al., 2016, 2019b). In other cases, however, several distinct species were discovered in what used to be treated as one widely distributed species (e.g., Hutsemékers & al., 2012; Medina & al., 2013; Patiño & al., 2017; Renner & al., 2017). In the genus *Pelekium* Mitt., for example, with several pantropical species, Norhazrina & al. (2016) detected high degrees of genetic diversity and phylogeographic structure. This was seen as evidence for *in situ* diversification within regions (mostly continents), which takes place at a faster rate than the intercontinental migration. The strong phylogeographic signal found in many bryophyte species at the intercontinental scale (Patiño & Vanderpoorten, 2018), along with the strong population genetic structuring observed in a number of continentally disjunct species (Désamoré & al., 2016; Vanderpoorten & al., 2019), is in line with the notion that speciation has a spatial scale that depends on both area and levels of gene flow (Kisel & Barraclough, 2010). Our results suggest that in *Epipterygium*, large geographic areas seem to be required to allow speciation in allopatry. The *E. tozeri* species complex consists of multiple overlooked species on the Eurasian and North American continents rather than one widespread Holarctic taxon, and the age estimates and biogeographic patterns fit to a history dominated by vicariance events. In the Macaronesian islands, however, no phylogeographic signal was detected, pointing to a much more recent and dynamic history among archipelagos, most likely driven by a number of LDD events, which must have played a role also in founding the not sequenced *Epipterygium* populations in Vanuatu and New Zealand.

Based on our morphological and molecular analyses, we congruently identified five overlooked species within the *E. tozeri* complex. Both of the methods we used for molecular species delimitation tend to overestimate the number of putative species (Carstens & al., 2013; Lang & al., 2015; Luo & al., 2018). Delineated entities consisting of only one or two haplotypes could either be ascribed to the model-implicit tendency for overestimation or to cryptic speciation which has been shown to be common among bryophytes in previous studies (e.g., Shaw, 2000, 2001; Feldberg & al., 2004; Buchbender & al., 2014). The benefit of species descriptions based only on molecular data has been discussed controversially (Carstens & al., 2013; Vanderpoorten & Shaw, 2014).

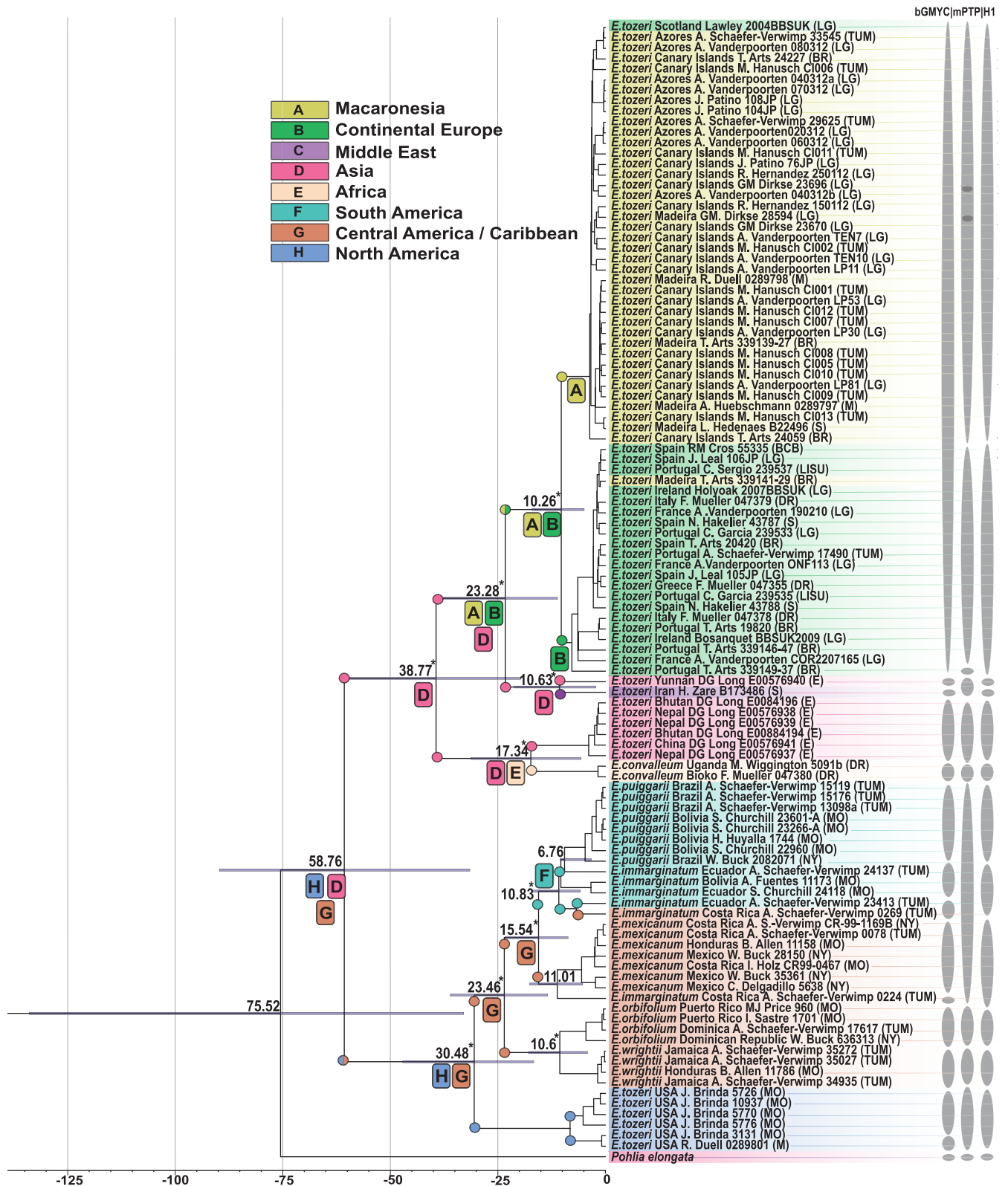


Fig. 3. Ancestral area distributions of *Epipterygium* inferred with DIVALIKE in BioGeoBEARS. Species names color-coded according to geographic origin of the specimens. Numbers above branches indicate best divergence time estimate according to a relaxed clock dating, blue bar indicates 95% highest posterior density. Rectangles below the branches indicate most likely ancestral states at nodes. The corner positions represent geographical ranges immediately after a dispersal or speciation event. Asterisks mark nodes with a posterior probability >0.95. The vertical bars indicate the estimated entities from the bGMYC, mPTP and our taxonomic hypothesis H1.

We therefore tried to set up a taxonomic treatment (H1) that addresses these aspects and identified two or more molecular entities as only one species if they have a sympatric distribution and overlapping morphology.

Our biogeographic analysis revealed a most likely origin of *Epipterygium* in Asia or in North/Central America. A dense family-wide sampling would be required to decide between these two options. The early split into an Old World and a New World clade, as well as perhaps a stepwise North to South colonization of the American regions, suggests that transcontinental LDD events are not too frequent in this genus. The close relationship of the African *E. convalleum* to Asian populations, however, is best interpreted as the result of a transcontinental LDD event. The colonizations of New Zealand and Vanuatu must have been the result of a transoceanic LDD event, but until specimens of *E. vanuatuicum* and *E. opararensis* can be sequenced, we are unable to determine the geographic origin of these LDDs. In contrast, the limited dispersal ability in American *Epipterygium* might be a result of scarce sporophyte production and widespread vegetative reproduction in the genus (Shaw, 1984; Fife & Shaw, 1990), including the production of perennial rhizoid-tubers (Arts & Nordhorn-Richter, 1986). Spores and specialized vegetative propagules are indeed thought to display complementary roles. Whereas spores might significantly contribute to LDD, specialized vegetative propagules are, due to the larger size and lack of release mechanisms, thought to mainly contribute to short-distance dispersal and population persistence (reviewed in Patiño & Vanderpoorten, 2018; but see Laenen & al., 2016). This reproductive strategy could have promoted allopatric speciation across the American continent, resulting in the six species accepted in the present study. A broader sampling, including more material, particularly from the African, Asian and the Pacific regions, would be required to obtain a more detailed understanding of the fine-scale evolutionary processes in *Epipterygium*.

Precise dating plays a key role in revealing the origin of new ecological niches or the role of vicariance versus dispersal in shaping distribution patterns (Villarreal & Renner, 2014). Unfortunately, fossil evidence of bryophytes is very scarce (Heinrichs & al., 2006, 2009), and average substitution rates are probably still the best option to date phylogenetic trees in most bryophyte groups. Here, we applied absolute nucleotide substitution rates derived from an extensive analysis across different groups of plants (Kay & al., 2006; Villarreal & Renner, 2014) that have been applied to a number of biogeographical bryophyte studies (e.g., Bechteler & al., 2017; Patiño & al., 2017; Vigalondo & al., 2019a). While such average rates are unlikely to represent accurately the specific situation of *Epipterygium*, the obtained ranges should give a good general estimate of the evolutionary time windows. While diversification within the Old World clade started 16–47 Ma, the New World species diversified approximately 19–60 Ma. In the New World, one possible scenario is that migration and diversification started in North America and continued via Central America and the West Indies. From

there, it seems the genus could have dispersed to tropical South America around 8–23 Ma, diversifying around 6–17 Ma. Our results, however, do not exclude the possibility of a South-North directionality (Fig. 3).

Moreover, our ancestral area reconstruction and dating analyses failed to provide support for the hypothesis that the western North America-western Europe disjunction in *E. tozeri* is a result of a LDD event via the North Atlantic Land Bridge (Tiffney, 2000). Instead, it is best explained as a product of vicariance and parallel evolution in both Europe and North America after the split of North America from Eurasia including or not dispersal across the Beringian Land Bridge (Tiffney & Manchester, 2001). The latter hypothesis, originally proposed by Axelrod (1975), postulated that European and North American lineages could have evolved from widespread mesic Madrean-Tethyan taxa through adaptations to dry climate regimes (Meusel, 1969; reviewed in Kadereit & Baldwin, 2012). Given that *Epipterygium* occurs in western North America, continental Europe and Macaronesia under oceanic (humid) climatic regimes, speciation within the *E. tozeri* complex seems to be a case of parallel allopatric evolution where a similar ecological niche is retained over evolutionary time (niche conservatism, sensu Wiens & Graham, 2005).

Indeed, the evolution of multiple local endemics in the Caribbean indicates that gene flow in the genus tends to be limited, facilitating allopatric speciation. In contrast to the situation in the Caribbean, we did not find a clear genetic structure within Macaronesia. This indicates that gene flow between the isolated Azores archipelago and Madeira, the Canary Islands and even Scotland is possible and likely not infrequent, limiting the potential for geographic speciation on any of the Macaronesian islands. The disjunct distribution pattern here involving the Macaronesian islands and the western fringe of Europe is not unusual in bryophytes, and forms the species-rich European Atlantic fringe bryophyte flora (Preston & Hill, 1999). Population genetic evidence based on coalescent demographic modelling suggests that this floristic element mainly assembled from Macaronesian ancestors during the most recent glacial–interglacial cycles, in particular from the mid to the Late Pleistocene (Patiño & al., 2015). This is a working hypothesis that remains to be tested in *Epipterygium*.

Our findings reinforce the idea that integrative taxonomic methods for species delimitation can help to recognize and split broadly distributed taxa into distinct species and analyze their historical biogeography. Our results add evidence to the mounting number of studies calling for the need of revisiting the species definitions of putative bryophyte species that exhibit such intercontinental distributions (Vigalondo & al., 2019a,b; reviewed in Patiño & Vanderpoorten, 2018). These, as the present study, have consistently incorporated different sources of information, ranging from morphology and molecular variation to geography, leaving other key life-history traits related to ecology and reproductive biology aside, mainly due to the lack of basic knowledge for the bulk of species. Therefore, we highlight the need to incorporate ecological, reproductive and dispersal data in order to shed

light on the mechanisms explaining the recurrent regional episodes of speciation, in particular in insular systems.

■ TAXONOMIC TREATMENT OF THE *EIPTERYGIUM TOZERI* COMPLEX

The type specimen of *Bryum tozeri* Grev. (*Tozer s.n.*, E barcode E00007536), the basionym of *E. tozeri*, in the Edinburgh Herbarium, consists of only two gametophytes, but the original description (Greville, 1827) is illustrated with six accurate pencil drawings of habitus, leaves and capsules of the species (<http://data.rbge.org.uk/herb/E00007536>). The type locality is in southwest England. Unfortunately, we could not sequence the type and also did not manage to obtain any topotypic material. Our geographically closest samples are from Ireland, included in the continental European clade. The description and photography of the type specimen also matches best plants from this group, which grow to up to 13 mm, whereas specimens of Macaronesian origin never exceed 4 mm in size. We therefore conclude that our continental European clade represents *Eipterygium tozeri* (Grev.) Lindb. and provide below formal descriptions for the remaining lineages formerly included in *E. tozeri*. Due to the lack of

sufficient plant material for detailed morphological investigation, we refrain from describing the Iranian population as a distinct species, even though this geographically isolated lineage seems to be clearly different at the molecular level. Though we were not able to obtain usable sequences from Japanese specimens, they showed a set of quantitative and qualitative morphological characters that clearly separate them from the continental European *E. tozeri* populations (e.g., median and marginal cell lengths, serration of perichaetial leaves). We therefore reinstate the name of *Eipterygium nagasakense* Broth. for the Japanese populations of *Eipterygium*.

Eipterygium tozeri (Grev.) Lindb. in Öfvers. Kongl. Vetensk.-Akad. Förh. 21(10): 577. 1865 (“1864”) ≡ *Bryum tozeri* Grev., Scott. Crypt. Fl. 5: t. 285. 1827 ≡ *Webera tozeri* (Grev.) Schimp., Coroll. Bryol. Eur.: 67. 1856 ≡ *Anisostichium tozeri* (Grev.) Mitt. in J. Proc. Linn. Soc., Bot. 7: 119. 1863 ≡ *Pohlia tozeri* (Grev.) Delogne in Ann. Soc. Belge Microscop. 9: 51. 1885 – Lectotype (designated by Shaw in Bryologist 87(2): 136. 1984); UNITED KINGDOM. Devonshire, River Dart; 1 Jul 1820, *J.S. Tozer s.n.* (E barcode E00007536 [digital image!]). Illustrated in Fig. 4.

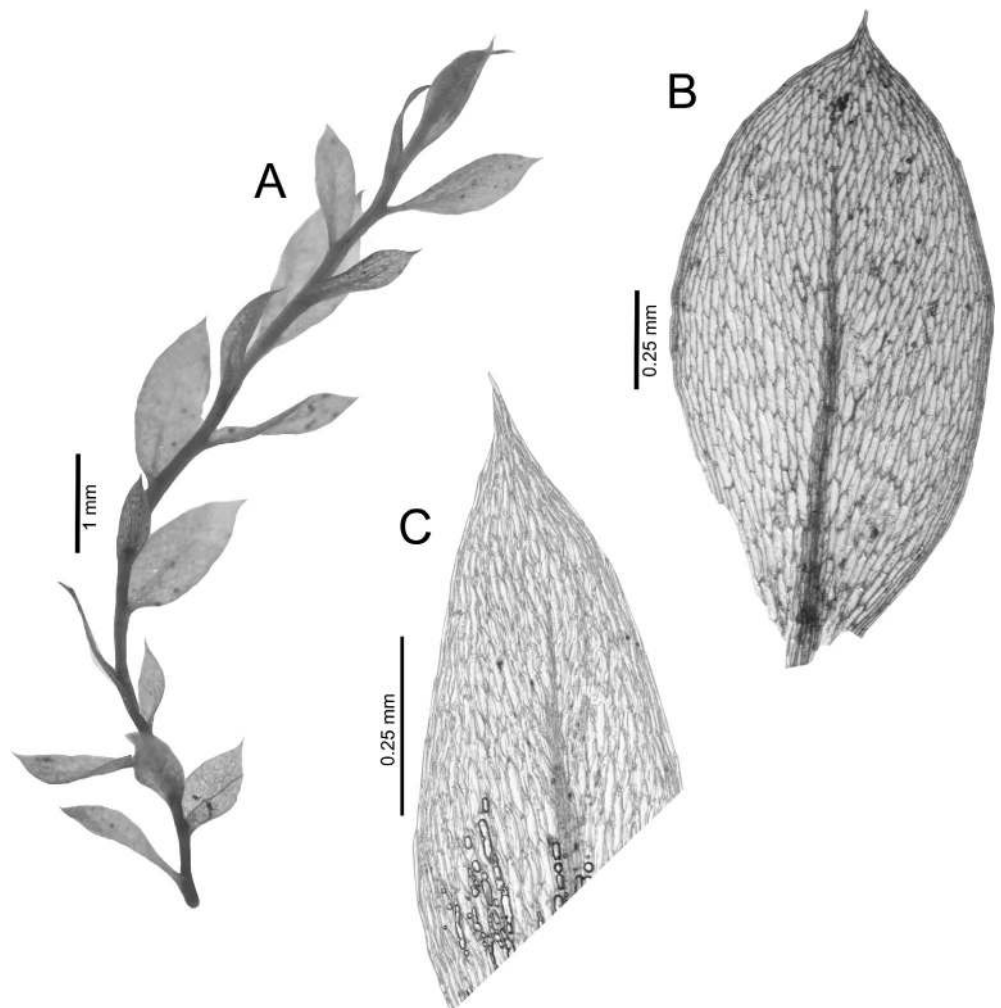


Fig. 4. *Eipterygium tozeri* (Grev.) Lindb. **A**, Habitus; **B**, Dorsal leaf; **C**, Perichaetial leaf apex.

Eipterygium atlanticum Hanusch, **sp. nov.** – Holotype: PORTUGAL. Azores, Terceira, Zentrale Nordküste, Wanderweg PR 2 Baías Agualva zwischen Quatro Ribeiras und Agualva, an Lavablock in kleiner Schlucht; 15 m; WGS84: 36°47.6–7'N, 27°11.5–8'W; *A. Schäfer-Verwimp* & *I. Verwimp*, 3 Jun 2012, Herb. *Schäfer-Verwimp* 33545 (TUM No. M2143!).

Diagnosis. – An *Eipterygium* species with short stems, gametophyte hardly exceeding 4 mm in size. Dorsal and ventral leaves dimorphic, one row of distinctly smaller ventral leaves. Dorsal leaves 4 to 5 per stem, obtuse to ovate, 1.5–2.1 mm long. Costa ending well before tip. Perichaetial leaves entire, non-serrate, median cells 90–150 µm long, 3 to 4 rows of marginal cells. Illustrated in Fig. 5.

Distribution. – Subtropical, oceanic climates. Atlantic islands (Azores, Madeira, Canary Islands), Scotland. The distribution on the British Isles needs to be investigated in more detail but the species does not seem to be a strict Macaronesian endemic.

Eipterygium biauratum Hanusch, **sp. nov.** – Holotype: U.S.A. California, California Department of Parks and Recreation, Big Basin Redwoods State Park, West Wadell Creek State Wilderness, along West Berry Creek near Golden and Silver Falls; 37.177655°N, 122.270708°W (WGS84), altitude: ca. 200 m, Coastal Redwood Forest,

on rock, sandstone, 29 Mar 2014, *John C. Brinda* 5770 (TUM No. M2144!).

Diagnosis. – A medium-sized *Eipterygium* species with stems ranging between 5 and 8 mm in size. Dull, bluish-green or sometimes pink plants. Dorsal and ventral leaves well developed, dimorphic, smaller ventral leaves arranged in 2 alternating rows. Dorsal leaves 1.0–2.2 mm long, oblong, or narrowly elliptical to lanceolate, acute, entire, non-serrate. Costa ending well before tip. Perichaetial leaf apex serrate. Dorsal leaf median cells 80–140 µm long, 20–30 µm wide, rhomboidal. Linear marginal cells forming a ± distinct border. Illustrated in Fig. 6.

Distribution. – North American Pacific coast. U.S.A., Canada.

Eipterygium oreophilum Hanusch, **sp. nov.** – Holotype: BHUTAN. Deothan District, 1 km east of Keri Gompa on Pemagatshel–Tshilingor road; 27°02'43.6"N, 91°26'02.4"E, altitude: ca. 2000 m, Evergreen *Quercus lamellosa* forest slopes, disturbed and grazed; on thin soil on vertical bank, 8 May 2011, *D.G. Long* & *K. Wangchuck s.n.* (E barcode E00884194!).

Diagnosis. – A smaller *Eipterygium* species with stems ranging between 3 and 5 mm in size. Dull, bluish-green or sometimes pink plants. Dorsal and ventral leaves scarcely dimorphic, Dorsal leaves 1–1.5 mm long, ovate, acute to

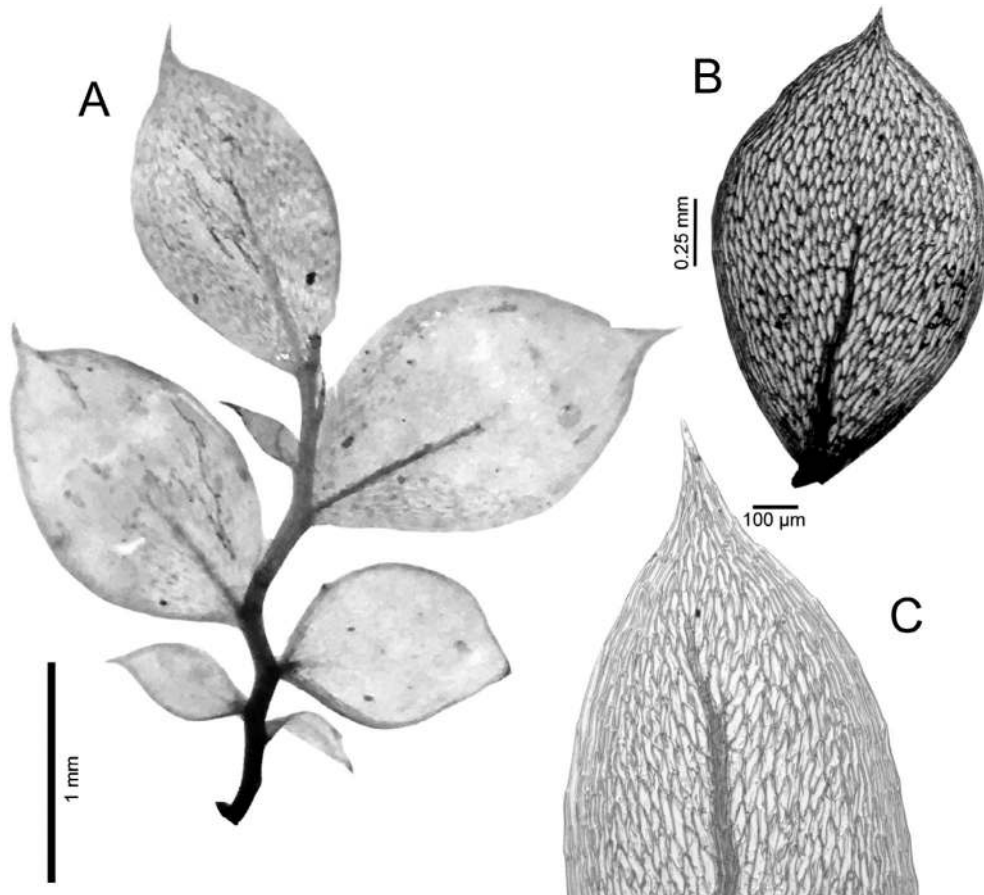


Fig. 5. *Eipterygium atlanticum* sp. nov. **A**, Habit; **B**, Dorsal leaf; **C**, Perichaetial leaf apex.

cuspidate, entire, non-serrate. Costa ending at half of lamina. Perichaetial leaves serrate to about half of the length, acute. Dorsal leaf median cells 60–110 μm long, 15–40 μm wide, rhomboidal. Linear marginal cells present forming a weak border. Illustrated in Fig. 7.

Distribution. – Himalaya. Bhutan, Nepal, China.

Note. – C. Müller (1901) described *E. falconeri* from Mussoorie, Uttarakhand, India (North-West Himalaya), which was later synonymized with *E. tozeri* (Van der Wijk & al., 1962). Despite the geographical proximity of collection sites, it seems unlikely that our new species *E. oreophilum* or *E. yunnanense* are conspecific to *E. falconeri*. We did not study the microscopical characters of the type specimen (*Duthie s.n.*, PC 2-D barcode PC0130926, <https://science.mnhn.fr/institution/mnhn/collection/pc/item/pc0130926>) but based on the description, the median cells of the species are distinctly narrower than those of *E. tozeri* (“[...] welche durch ein weit engeres Blattnetz sogleich von *E. tozeri* abweicht.”). This is in contrast to what we find in both *E. oreophilum* and *E. yunnanense*, where the cells are much wider than in *E. tozeri* (length-to-width ratio of 3.37 ± 0.47 and 3.87 ± 0.57 , respectively, compared to a ratio of 5.01 ± 1.05 in *E. tozeri*).

Eipterygium yunnanense Hanusch, **sp. nov.** – Holotype: CHINA. Yunnan Province, Tengchong Xian, Longchuan Jiang valley along roads from Qushi to Tengchong, west branch of Longchuan Jiang at Xiangyangqiao bridge; $25^{\circ}12'42''\text{N}$, $98^{\circ}34'48''\text{E}$, altitude ca. 1471 m, wooded slopes above river with *Alnus nepalensis* and scrub, on soil on shady roadside rocks, 25 Oct 2003, *D.G. Long s.n.* (E barcode E00576940!).

Diagnosis. – A large *Eipterygium* species with stems ranging between 7 and 9 mm in size. Dull, bluish-green or sometimes pink plants. Dorsal and ventral leaves scarcely dimorphic, dorsal leaves 1.6–2.1 mm long, ovate, acute to cuspidate, entire, non-serrate. Costa ending at half of lamina. Perichaetial leaves serrate to about half of the length, acute. Dorsal leaf median cells 110–125 μm long, 25–40 μm wide, rhomboidal; 4–8 rows of linear marginal cells forming a very distinct border. Illustrated in Fig. 8.

Distribution. – Asia. China, Yunnan.

Eipterygium nagasakense Broth. in Hedwigia 38: 217. 1899 – Type: JAPAN. Nagasaki, 14 Jan 1861, *M.E. Wichura 1383a* (PC 2-D barcode PC0130916 [digital image!]).

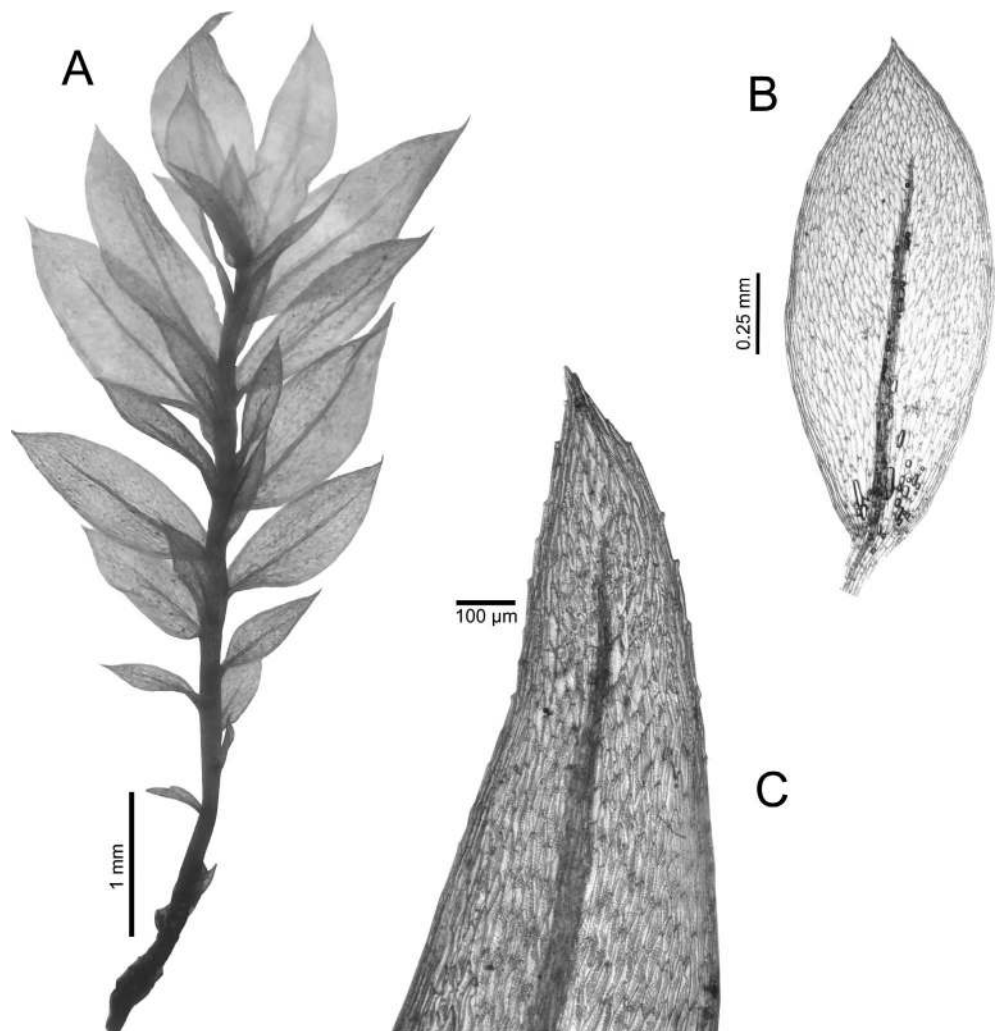


Fig. 6. *Eipterygium biauratum* sp. nov. **A**, Habitus; **B**, Dorsal leaf; **C**, Perichaetial leaf apex.

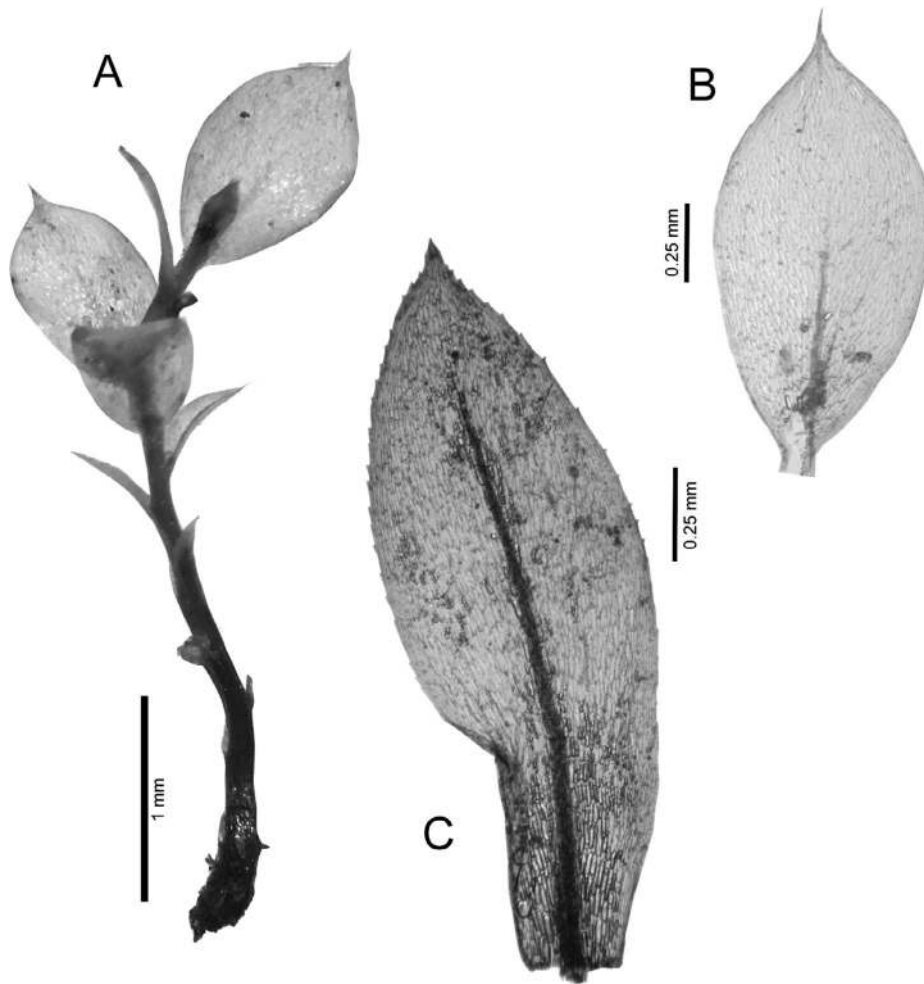


Fig. 7. *Eipterygium oreophilum* sp. nov. A, Habitus; B, Dorsal leaf; C, Perichaetial leaf apex.

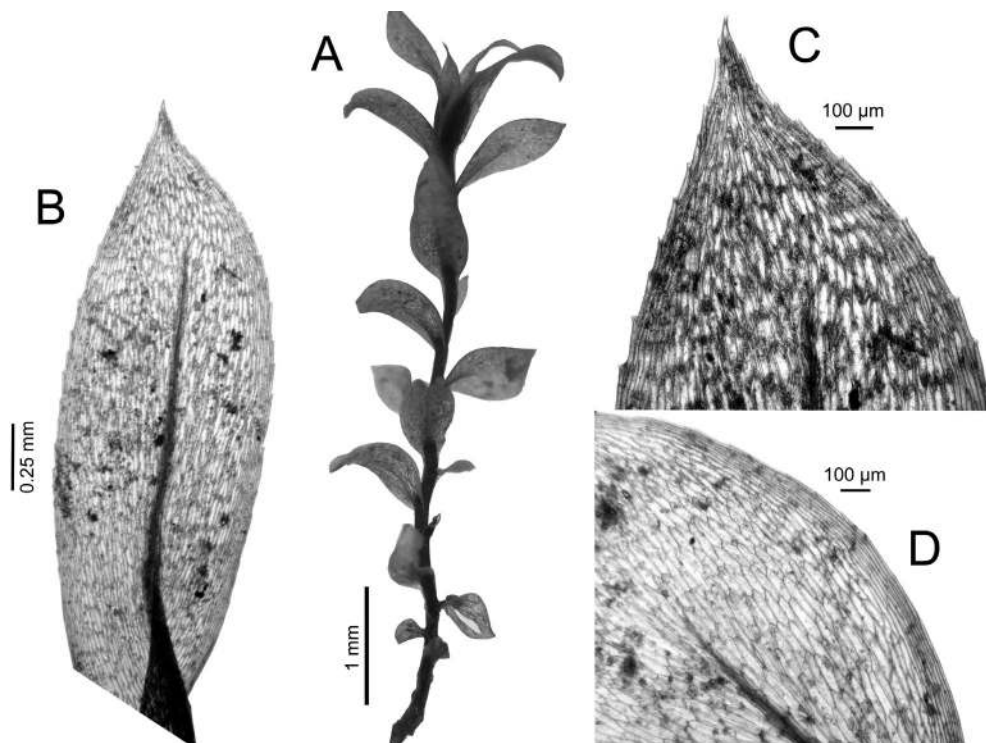


Fig. 8. *Eipterygium yunnanense* sp. nov. A, Habitus; B, Perichaetial leaf; C, Perichaetial leaf apex; D, Marginal cells of dorsal leaf.

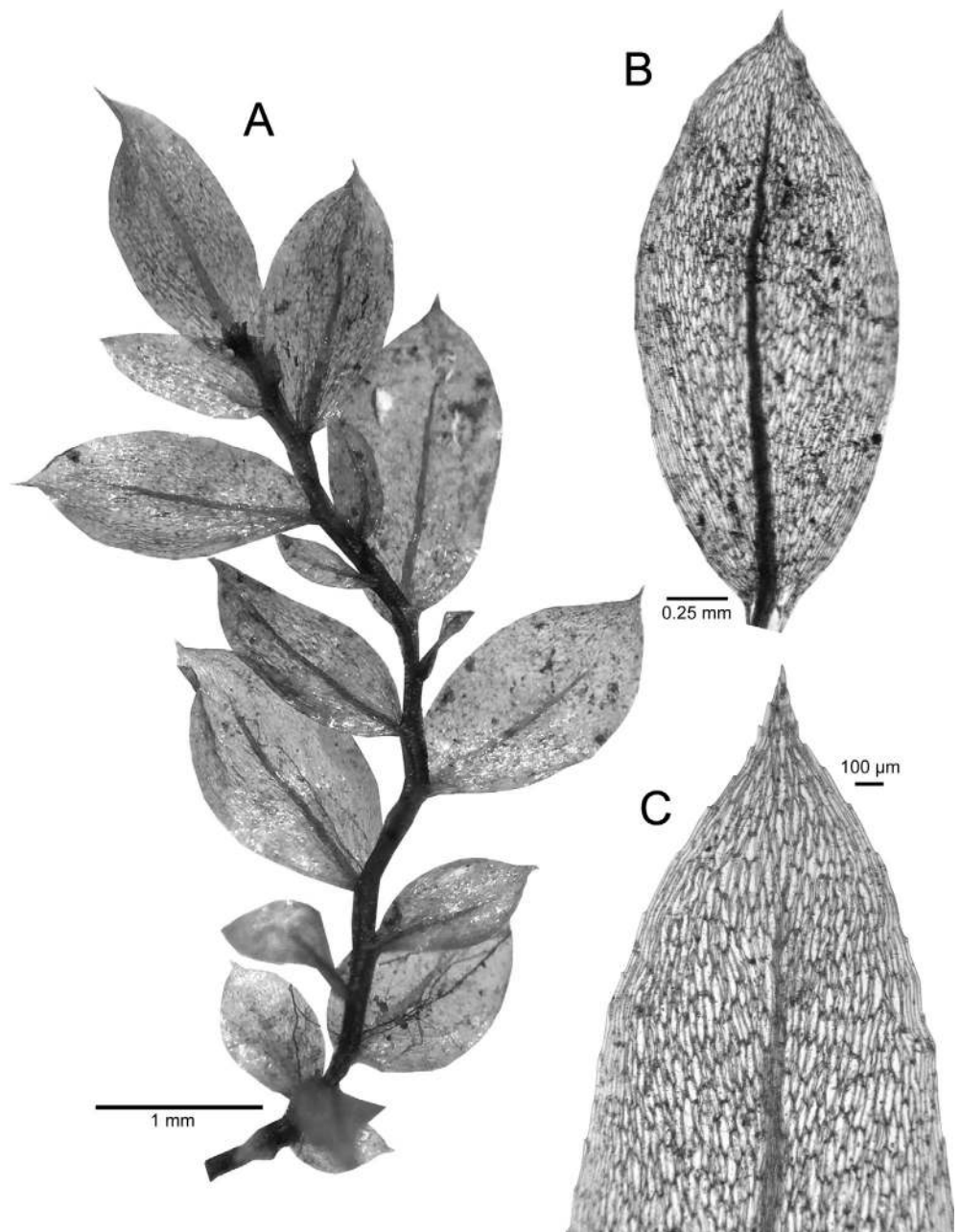


Fig. 9. *Epipterygium nagasakense*.
A, Habitus; B, Dorsal leaf; C, Perichaetial leaf apex.

Diagnosis. – A large *Epipterygium* species with stems ranging between 5 and 10 mm in size. Pale reddish plants. Dorsal and ventral leaves complanate. Dorsal leaves 1.6–2.1 mm long, ovate, acuminate. Upper dorsal leaves slightly serrate at leaf tip. Costa ending well below leaf apex. Perichaetial leaves serrate at leaf tip, acute. Dorsal leaf median cells 100–125 μm long, about 25 μm wide, rhomboidal. Up to 5 rows of linear marginal cells forming a border of the same colour. Illustrated in Fig. 9.

Distribution. – Asia. Japan.

Key to the species of *Epipterygium*

Small or very small, delicate, cespitose or loosely tufted, pale green, reddish-green to yellowish or white, beamless or shiny plants. Stems simple, reddish to green, sometimes

branched at basis, erect to decumbent or reclining. Rhizoids forming at stem base. Leaves dimorphous, sometimes less distinctly on fertile stems. Dorsal leaves shorter, more tapered, obliquely protruding from stem in one or two rows. Leaves distant at base, more crowded and larger at stem tips, loosely spreading, thin, elliptic, ovate or obovate to oblong-lanceolate, acute or abruptly short-acuminate, more or less decurrent. Leaf margins entire, with a distinct or less marked, often reddish border. Perichaetial leaf apex sometimes serrate. Costa slender, extending one-half to five-sixths of the leaf length. Cells pale, lax, delicate, thin-walled, rhomboidal to irregularly rhomboidal, narrower and longer at leaf margins forming a more or less distinct border.

This key covers all species examined in the present study. Five species of the genus are not covered by this key due to

lack of material: *E. brasiliense* E.B.Bartram, *E. koelzii* H.Rob., *E. mandonii* (Müll.Hal.) Paris, *E. rigidum* Lindb., and *E. vanuatuicum* H.A.Mill.

1. Stems with one row of smaller ventral leaves; Old World2
1. Stems with two or no rows of smaller ventral leaves; New World7
2. Gametophyte up to 5 mm long.....3
2. Gametophyte more than 5 mm long.....5
3. Plants complanate, green to red; broadly ovate lateral leaves, 1.5–2.1 mm in length, median cell length 90–150 µm; oceanic climate; western Europe, Macaronesia *E. atlanticum*
3. Plants not complanate, leaves ± spreading; Africa, Asia4
4. Lateral leaves up to 1.5 mm long, perichaetial leaf tip serrate; Himalayas: Bhutan, Nepal, China *E. oreophilum*
4. Lateral leaves up to 3.3 mm long, perichaetial leaf tip not serrate; Africa: Bioko, Uganda..... *E. convalleum*
5. Perichaetial leaves not serrate, leaves not distinctly bordered, median cell length up to 225 µm; Europe: Mediterranean, Madeira *E. tozeri*
5. Perichaetial leaves serrate, leaves distinctly bordered, median cell length up to 130 µm, Asia: Japan, China 6
6. Costa ending just below apex, median cells 25–30 µm wide; Japan..... *E. nagasakense*
6. Costa ending well below apex, median cells 28–40 µm wide; China: Yunnan, subtropical highland climate *E. yunnanense*
7. Plants strongly complanate and dimorphous-foliolate or non-dimorphous foliolate, leaves strongly or weakly bordered, red or pale green leaves; New Zealand, West Indies8
7. Plants weakly or sometimes strongly complanate and dimorphous foliolate, green or pink; median cells 8–30 µm wide; temperate and tropical North, Central or South America..... 10
8. Gametophyte up to 15 mm long, pale green plants, leaves monomorphic; New Zealand..... *E. opararensense*
8. Gametophyte up to 30 mm long, reddish, rarely green plants, leaves dimorphic; West Indies9
9. Median cells regularly rhomboidal, lateral leaves broadly elliptical to oblong; West Indies, Cuba, Jamaica *E. wrightii*
9. Median cells irregularly rhomboidal, lateral leaves orbicular to ovate; West Indies and northern South America *E. orbifolium*
10. Plants glossy, green; leaves scarcely bordered; cells 8–16 µm wide; Central America *E. mexicanum*
10. Plants dull, bluish-green to pink; leaves often bordered; cells 16–30 µm wide11
11. Plants scarcely or not at all complanate or dimorphous-foliolate, leaves lanceolate; temperate America *E. biauratum*

11. Plants weakly or often strongly complanate and dimorphous-foliolate, leaves elliptical; tropical America12
12. Lower leaves orbicular to ovate, not distinctly bordered; tropical America, South America *E. puiggarii*
12. Lower leaves elliptical, plants weakly or often strongly complanate and dimorphous-foliolate; tropical America *E. immarginatum*

■ AUTHOR CONTRIBUTIONS

HS and JP supervised the project. MH and JP conceived sample acquisition and laboratory work. MH, EMO, JP and HS performed the analysis. MH drafted the manuscript and species descriptions. All authors provided critical feedback and helped shape the research, analysis and manuscript. — MH, <https://orcid.org/0000-0001-7228-1276>; EMO, <https://orcid.org/0000-0001-8052-1671>; JP, <https://orcid.org/0000-0001-5532-166X>; HS, <https://orcid.org/0000-0001-7231-3987>

■ ACKNOWLEDGEMENTS

We thank A. Höwener for help in the lab and the curators of the herbaria BSM, DR, E, LG, LISU, M, MO, NY, S, TUM and A. Schäfer-Verwimp (Herdwangen-Schönach, Germany) for material and permission to extract DNA. We thank A. Vanderpoorten (Liège) for help with sampling, sample identification, and insightful comments during the study. Jonathan Shaw greatly stimulated with initial discussions. JP was funded by the MINECO through the Juan de la Cierva Program-Incorporation (JICI-2014-19691) and Ramón y Cajal Program (RYC-2016-20506), and Marie Skłodowska-Curie COFUND, Researchers' Night and Individual Fellowships Global (MSCA grant agreement No 747238, "UNIS-LAND"). We thank R. Medina for comments on the manuscript. Open access funding enabled and organized by Projekt DEAL.

■ LITERATURE CITED

- Aberer, A.J., Krompass, D. & Stamatakis, A. 2013. Pruning rogue taxa improves phylogenetic accuracy: An efficient algorithm and webservice. *Syst. Biol.* 62: 162–166. <https://doi.org/10.1093/sysbio/sys078>
- Akaike, H. 1974. A new look at the statistical model identification. *IEEE Trans. Automatic Control* 19: 716–723. <https://doi.org/10.1109/TAC.1974.1100705>
- Arts, T. & Nordhorn-Richter, G. 1986. *Epipterygium tozeri* in Europe, its distribution and vegetative propagation. *J. Bryol.* 14: 91–97. <https://doi.org/10.1179/jbr.1986.14.1.91>
- Axelrod, D.I. 1958. Evolution of the madro-tertiary geoflora. *Bot. Rev. (Lancaster)* 24: 433–509. <https://doi.org/10.1007/BF02872570>
- Axelrod, D.I. 1975. Evolution and biogeography of Madrean-Tethyan sclerophyll vegetation. *Ann. Missouri Bot. Gard.* 62: 280–334. <https://doi.org/10.2307/2395199>
- Bartram, E.B. 1952. New mosses from southern Brazil. *J. Wash. Acad. Sci.* 42: 178–182.
- Bechteler, J., Schäfer-Verwimp, A., Lee, G.E., Feldberg, K., Pérez-Escobar, O.A., Pócs, T., Peralta, D.F., Renner, M.A.M. & Heinrichs, J. 2017. Geographical structure, narrow species ranges, and Cenozoic diversification in a pantropical clade of epiphyllous leafy liverworts. *Ecol. Evol.* 7: 638–653. <https://doi.org/10.1002/ece3.2656>
- Bizot, M. 1971. Rectifications. *Rev. Bryol. Lichénol.* 38: 638–653.
- Brotherus, V.F. 1892. Enumeratio muscorum Caucasi. *Acta Soc. Sci. Fenn.* 19: 1–170.

- Brotherus, V.F.** 1909. Acrocarpi. Pp. 283–700 in: Engler, A. & Prantl, K. (eds.), *Die natürlichen Pflanzenfamilien*, I(3). Leipzig: Engelmann. <https://doi.org/10.5962/bhl.title.4635>
- Buchbender, V., Hespánhol, H., Krug, M., Sergio, C., Seneca, A., Maul, K., Hedenäs, L. & Quandt, D.** 2014. Phylogenetic reconstructions of the Hedwigiaceae reveal cryptic speciation and hybridisation in *Hedwigia*. *Bryophyte Diversity Evol.* 36: 1–21.
- Caparrós, R., Lara, F., Draper, I., Mazimpaka, V. & Garilleti, R.** 2016. Integrative taxonomy sheds light on an old problem: The *Ulotia crista* complex (Orthotrichaceae, Musci). *Bot. J. Linn. Soc.* 180: 427–451. <https://doi.org/10.1111/boj.12397>
- Carstens, B.C., Pelletier, T.A., Reid, N.M. & Satler, J.D.** 2013. How to fail at species delimitation. *Molec. Ecol.* 22: 4369–4383. <https://doi.org/10.1111/mec.12413>
- Charif, D. & Lobry, J.R.** 2007. SeqinR 1.0-2: A contributed package to the R Project for Statistical Computing devoted to biological sequences retrieval and analysis. Pp. 207–232 in: Bastolla, U., Porto, M., Roman, H.E. & Vendruscolo, M. (eds.), *Structural approaches to sequence evolution: Molecules, networks, populations*. New York: Springer. https://doi.org/10.1007/978-3-540-35306-5_10
- Cheng, T., Xu, C., Lei, L., Li, C., Zhang, Y. & Zhou, S.** 2016. Barcoding the kingdom Plantae: New PCR primers for ITS regions of plants with improved universality and specificity. *Molec. Ecol. Resources* 16: 138–149. <https://doi.org/10.1111/1755-0998.12438>
- Cox, C.J. & Hedderson, T.A.J.** 1999. Phylogenetic relationships among the ciliate arthrodontous mosses: Evidence from chloroplast and nuclear DNA sequences. *Pl. Syst. Evol.* 215: 119–139. <https://doi.org/10.1007/BF00984651>
- Crum, H.** 1967. Studies in North American Bryaceae I–II. *Bryologist* 70: 106–110. <https://doi.org/10.2307/3241146>
- Crundwell, A.C., Crum, H.A. & Anderson, L.E.** 1982. Mosses of eastern North America. *Bryologist* 85: 173–175. <https://doi.org/10.2307/3243165>
- Davison, P.G., Smith, D.K., Feldberg, K., Lindner, M. & Heinrichs, J.** 2006. *Plagiochila punctata* (Plagiochilaceae) in Tennessee, new to North America. *Bryologist* 109: 242–246. [https://doi.org/10.1639/0007-2745\(2006\)109\[242:pppitt\]2.0.co;2](https://doi.org/10.1639/0007-2745(2006)109[242:pppitt]2.0.co;2)
- Désamoré, A., Patiño, J., Mardulyn, P., Mcdaniel, S.F., Zanatta, F., Laenen, B. & Vanderpoorten, A.** 2016. High migration rates shape the postglacial history of amphiatlantic bryophytes. *Molec. Ecol.* 25: 5568–5584. <https://doi.org/10.1111/mec.13839>
- Dusén, P.** 1895. New and some little known Mosses from the West Coast of Africa II. *Kongl. Svenska Vetensk. Acad. Handl.* 28(3): 1–56.
- Feldberg, K., Groth, H., Wilson, R., Schäfer-Verwimp, A. & Heinrichs, J.** 2004. Cryptic speciation in *Herbertus* (Herbertaceae, Jungermanniopsida): Range and morphology of *Herbertus sendtneri* inferred from nrITS sequences. *Pl. Syst. Evol.* 249: 247–261. <https://doi.org/10.1007/s00606-004-0221-4>
- Fife, A.J. & Knightbridge, P.** 2005. *Distribution of the very rare moss Epipterygium opararensense and recommendations for track upgrades at Oparara*. DOC Research & Development Series 221. Wellington: Science & Technical Publishing Department of Conservation. <http://www.doc.govt.nz/Documents/science-and-technical/drds221.pdf>
- Fife, A.J. & Shaw, A.J.** 1990. *Epipterygium* (Musci: Bryaceae) new to Australasia, with the description of *E. opararensense*, sp. novo. *New Zealand J. Bot.* 28: 375–379. <https://doi.org/10.1080/0028825X.1990.10412325>
- Fleischer, M.** 1922. Kritische Revision der Carl Müllerschen Laubmoosgattungen. *Hedwigia* 63: 209–216.
- Fritsch, P.W.** 2001. Phylogeny and biogeography of the flowering plant genus *Styrax* (Styracaceae) based on chloroplast DNA restriction sites and DNA sequences of the internal transcribed spacer region. *Molec. Phylogen. Evol.* 19: 387–408. <https://doi.org/10.1006/mpev.2001.0933>
- Greville, R.K.** 1827. *Scottish cryptogamic flora*, vol. 5. Edinburgh: Maclachlan & Stewart. <https://bibdigital.rjb.csic.es/idurl/1/11454>
- Grummer, J.A., Bryson, R.W. & Reeder, T.W.** 2014. Species delimitation using bayes factors: Simulations and application to the *Sceloporus scalaris* species group (Squamata: Phrynosomatidae). *Syst. Biol.* 63: 119–133. <https://doi.org/10.1093/sysbio/syt069>
- Heinrichs, J., Lindner, M., Groth, H., Hentschel, J., Feldberg, K., Renker, C., Engel, J.J., Konrat, M. von, Long, D.G. & Schneider, H.** 2006. Goodbye or welcome Gondwana? – Insights into the phylogenetic biogeography of the leafy liverwort *Plagiochila* with a description of *Proskauera*, gen. nov. (Plagiochilaceae, Jungermanniales). *Pl. Syst. Evol.* 258: 227–250. <https://doi.org/10.1007/s00606-006-0411-3>
- Heinrichs, J., Hentschel, J., Feldberg, K., Bombosch, A. & Schneider, H.** 2009. Phylogenetic biogeography and taxonomy of disjunctly distributed bryophytes. *J. Syst. Evol.* 47: 497–508. <https://doi.org/10.1111/j.1759-6831.2009.00028.x>
- Hileman, A., Lena, C. & Michael, C.** 2001. Phylogeny and biogeography of the Arbutioideae (Ericaceae): Implications for the Madrean-Tethyan hypothesis. *Syst. Bot.* 26: 131–143. [https://doi.org/10.1043/0363-6445\(2001\)026<0131](https://doi.org/10.1043/0363-6445(2001)026<0131)
- Hoang, D.T., Chernomor, O., Haeseler, A. von, Minh, B.Q. & Vinh, L.S.** 2018. UFBoot2: Improving the ultrafast bootstrap approximation. *Molec. Biol. Evol.* 35: 518–522. <https://doi.org/10.1093/molbev/msx281>
- Holyoak, D.T. & Pedersen, N.** 2007. Conflicting molecular and morphological evidence of evolution within the Bryaceae (Bryopsida) and its implications for generic taxonomy. *J. Bryol.* 29: 111–124. <https://doi.org/10.1179/174328207X189198>
- Huelsenbeck, J.P. & Ronquist, F.** 2001. MRBAYES: Bayesian inference of phylogenetic trees. *Bioinformatics* 17: 754–755. <https://doi.org/10.1093/bioinformatics/17.8.754>
- Hutsemékers, V., Vieira, C.C., Vanderpoorten, A., Huttunen, S. & Ros, R.M.** 2012. Morphology informed by phylogeny reveals unexpected patterns of species differentiation in the aquatic moss *Rhynchostegium riparioides* s.l. *Molec. Phylogen. Evol.* 62: 748–755. <https://doi.org/10.1016/j.ympev.2011.11.014>
- Huttunen, S., Hedenäs, L., Ignatov, M.S., Devos, N. & Vanderpoorten, A.** 2008. Origin and evolution of the Northern Hemisphere disjunction in the moss genus *Homalothecium* (Brachytheciaceae). *Amer. J. Bot.* 95: 720–730. <https://doi.org/10.3732/ajb.2007407>
- Kadereit, J.W. & Baldwin, B.G.** 2012. Western Eurasian–western North American disjunct plant taxa: The dry-adapted ends of formerly widespread North temperate mesic lineages—and examples of long-distance dispersal. *Taxon* 61: 3–17. <https://doi.org/10.1002/tax.611001>
- Kapli, P., Lutteropp, S., Zhang, J., Kobert, K., Pavlidis, P., Stamatakis, A. & Flouri, T.** 2017. Phylogenetics multi-rate Poisson tree processes for single-locus species delimitation under maximum likelihood and Markov chain Monte Carlo. *Bioinformatics* 33: 1630–1638. <https://doi.org/10.1093/bioinformatics/btx025>
- Kay, K.M., Whittall, J.B. & Hodges, S.A.** 2006. A survey of nuclear ribosomal internal transcribed spacer substitution rates across angiosperms: An approximate molecular clock with life history effects. *B. M. C. Evol. Biol.* 6: 1–9. <https://doi.org/10.1186/1471-2148-6-36>
- Kisel, Y. & Barraclough, T.G.** 2010. Speciation has a spatial scale that depends on levels of gene flow. *Amer. Naturalist* 175: 316–334. <https://doi.org/10.1086/650369>
- Kreier, H.-P., Mahr, F., Schmidt, A.R., Shaw, A.J., Konrat, M. von, Zhu, R.-L., Shaw, B., Feldberg, K., Heinrichs, J. & Bombosch, A.** 2010. Phylogeny of the leafy liverwort *Platidium*: Cryptic speciation and shared haplotypes between the Northern and Southern Hemispheres. *Molec. Phylogen. Evol.* 57: 1260–1267. <https://doi.org/10.1016/j.ympev.2010.10.002>

- Kyrkjeeide, M.O., Hassel, K., Flatberg, K.I., Shaw, A.J., Brochmann, C. & Stenøien, H.K. 2016. Long-distance dispersal and barriers shape genetic structure of peatmosses (*Sphagnum*) across the Northern Hemisphere. *J. Biogeogr.* 43: 1215–1226. <https://doi.org/10.1111/jbi.12716>
- Laenen, B., Machac, A., Gradstein, S.R., Shaw, B., Patiño, J., Désamoré, A., Goffinet, B., Cox, C.J., Shaw, A.J. & Vanderpoorten, A. 2016. Geographical range in liverworts: Does sex really matter? *J. Biogeogr.* 43: 627–635. <https://doi.org/10.1111/jbi.12661>
- Lanfear, R., Frandsen, P.B., Wright, A.M., Senfeld, T. & Calcott, B. 2017. Partitionfinder 2: New methods for selecting partitioned models of evolution for molecular and morphological phylogenetic analyses. *Molec. Biol. Evol.* 34: 772–773. <https://doi.org/10.1093/molbev/msw260>
- Lang, A.S., Bocksberger, G. & Stech, M. 2015. Phylogeny and species delimitations in European *Dicranum* (Dicranaceae, Bryophyta) inferred from nuclear and plastid DNA. *Molec. Phylog. Evol.* 92: 217–225. <https://doi.org/10.1016/j.ympev.2015.06.019>
- Lartillot, N. & Philippe, H. 2006. Computing Bayes factors using thermodynamic integration. *Syst. Biol.* 55: 195–207. <https://doi.org/10.1080/10635150500433722>
- Lewis, L.R., Rozzi, R. & Goffinet, B. 2014. Direct long-distance dispersal shapes a New World amphitropical disjunction in the dispersal-limited dung moss *Tetraplodon* (Bryopsida: Splachnaceae). *J. Biogeogr.* 41: 2385–2395. <https://doi.org/10.1111/jbi.12385>
- Lindberg, S.O. 1862. Om ett nytt släkte, *Epipterygium*, bland bladmossorna. *Öfvers. Kongl. Vetensk.-Akad. Förh.* 19: 599–609.
- Lindberg, S.O. 1864. Om bladmossornas locklösa former. *Öfvers. Kongl. Vetensk.-Akad. Förh.* 21: 575–589.
- Luo, A., Ling, C., Ho, S.Y.W. & Zhu, C.D. 2018. Comparison of methods for molecular species delimitation across a range of speciation scenarios. *Syst. Biol.* 67: 830–846. <https://doi.org/10.1093/sysbio/syy011>
- Matzke, N.J. 2013. Probabilistic historical biogeography: New models for founder-event speciation, imperfect detection, and fossils allow improved accuracy and model-testing. *Frontiers Biogeogr.* 5(4). <https://doi.org/10.21425/f5fbg19694>
- Matzke, N.J. 2014. Model selection in historical biogeography reveals that founder-event speciation is a crucial process in island clades. *Syst. Biol.* 63: 951–970. <https://doi.org/10.1093/sysbio/syu056>
- Medina, R., Lara, F., Goffinet, B., Garilleti, R. & Mazimpaka, V. 2012. Integrative taxonomy successfully resolves the pseudo-cryptic complex of the disjunct epiphytic moss *Orthotrichum consimile* s.l. (Orthotrichaceae). *Taxon* 61: 1180–1198. <https://doi.org/10.1002/tax.616002>
- Medina, R., Lara, F., Goffinet, B., Garilleti, R. & Mazimpaka, V. 2013. Unnoticed diversity within the disjunct moss *Orthotrichum tenellum* s.l. validated by morphological and molecular approaches. *Taxon* 62: 1133–1152. <https://doi.org/10.12705/626.15>
- Meusel, H. 1969. Beziehungen in der Florendifferenzierung von Eurasien und Nordamerika. *Flora* 158: 537–564. [https://doi.org/10.1016/s0367-1801\(17\)30241-7](https://doi.org/10.1016/s0367-1801(17)30241-7)
- Miller, H.A. 1988. Pacific Bryophytes: 4. *Epipterygium* in southern Melanesia. *Syst. Bot.* 13: 133–137. <https://doi.org/10.2307/2419249>
- Milne, R.I. 2006. Northern Hemisphere plant disjunctions: A window on tertiary land bridges and climate change? *Ann. Bot. (Oxford)* 98: 465–472. <https://doi.org/10.1093/aob/mcl148>
- Milne, R.I. & Abbott, R.J. 2002. The origin and evolution of tertiary relict floras. *Advances Bot. Res.* 38: 281–314. [https://doi.org/10.1016/S0065-2296\(02\)38033-9](https://doi.org/10.1016/S0065-2296(02)38033-9)
- Minh, B.Q., Trifinopoulos, J., Schrempf, D. & Schmidt, H.A. 2019. IQ-TREE version 2.0: Tutorials and Manual; Phylogenomic software by maximum likelihood. <http://www.iqtree.org/doc/iqtree-doc.pdf>
- Mitten, G. 1871. Musci Austro-Americani; sive Enumeratio Muscorum omnium Austro-Americanorum mihi hucusque cognitorum, eorum praecipue in terris Amazonicis Andinisque Ricardo Spruceo lectorum. *J. Linn. Soc., Bot.* 12: 1–630. <https://doi.org/10.1111/j.1095-8339.1871.tb00633.x>
- Monaghan, M.T., Wild, R., Elliot, M., Fujisawa, T., Balke, M., Inward, D.J.G., Lees, D.C., Ranaivosolo, R., Eggleton, P., Barraclough, T.G. & Vogler, A.P. 2009. Accelerated species inventory on Madagascar using coalescent-based models of species delineation. *Syst. Biol.* 58: 298–311. <https://doi.org/10.1093/sysbio/syp027>
- Müller, C. 1879. Musci Fendleriani Venezuelenses. *Linnaea* 42: 461–503.
- Müller, C. 1897a. Bryologia Guatemalensis. *Bull. Herb. Boissier* 5: 171–220.
- Müller, C. 1897b. Prodromus Bryologiae Boliviana. *Nuovo Giorn. Bot. Ital.* 4: 5–113.
- Müller, C. 1901. *Genera Muscorum frondosorum*. Leipzig: Kummer. <https://bibdigital.rjb.csic.es/idurl/1/9970>
- Müller, J., Müller, K., Neinhuis, C. & Quandt, D. 2005. PhyDE-Phylogenetic Data Editor. Program distributed by the authors. <http://www.phyde.de>
- Müller, K. 2005. SeqState: Primer design and sequence statistics for phylogenetic DNA datasets. *Appl. Bioinf.* 4: 65–69. <https://doi.org/10.2165/00822942-200504010-00008>
- Naimi, B., Hamm, N.A.S., Groen, T.A., Skidmore, A.K. & Toxopeus, A.G. 2014. Where is positional uncertainty a problem for species distribution modelling? *Ecography* 37: 191–203. <https://doi.org/10.1111/j.1600-0587.2013.00205.x>
- Newton, A.E., Hedderson, T.A.J., Duckett, J.G., Goffinet, B., Wheeler, J.A., Cox, C.J. & Mishler, B.D. 2006. Evolution of the major Moss lineages: Phylogenetic analyses based on multiple gene sequences and morphology. *Bryologist* 103: 187–211. [https://doi.org/10.1639/0007-2745\(2006\)103\[0187:eotmml\]2.0.co;2](https://doi.org/10.1639/0007-2745(2006)103[0187:eotmml]2.0.co;2)
- Nguyen, L.T., Schmidt, H.A., Haeseler, A. von & Minh, B.Q. 2015. IQ-TREE: A fast and effective stochastic algorithm for estimating maximum-likelihood phylogenies. *Molec. Biol. Evol.* 32: 268–274. <https://doi.org/10.1093/molbev/msu300>
- Nishiyama, T. & Kato, M. 1999. Molecular phylogenetic analysis among bryophytes and tracheophytes based on combined data of plastid coded genes and the 18S rRNA gene. *Molec. Biol. Evol.* 16: 1027–1036. <https://doi.org/10.1093/oxfordjournals.molbev.a026192>
- Norhazrina, N., Vanderpoorten, A., Hedenäs, L. & Patiño, J. 2016. What are the evolutionary mechanisms explaining the similar species richness patterns in tropical mosses? Insights from the phylogeny of the pantropical genus *Pelekium*. *Molec. Phylog. Evol.* 105: 139–145. <https://doi.org/10.1016/j.ympev.2016.08.008>
- Ochi, H. 1985. An annotated list of Mosses of the subfamily Bryoidae in South, Southeast and East Asia. *J. Fac. Educ. Tottori Univ., Nat. Sci.* 34: 41–96.
- Ogilvie, H.A., Bouckaert, R.R. & Drummond, A.J. 2017. StarBEAST2 brings faster species tree inference and accurate estimates of substitution rates. *Molec. Biol. Evol.* 34: 2101–2114. <https://doi.org/10.1093/molbev/msx126>
- Pacak, A. & Szweykowska-Kulińska, Z. 2000. Molecular data concerning allopolyploid character and the origin of chloroplast and mitochondrial genomes in the liverwort species *Pellia borealis*. *J. Pl. Biotechnol.* 2: 101–108.
- Paris, E.G. 1900. *Index bryologicus*, supplementum primum. Mémoires l'Herbier Boissier. Genève [Geneva] & Bale [Basel]: Georg & Cie. <https://bibdigital.rjb.csic.es/idurl/1/11432>
- Patiño, J. & Vanderpoorten, A. 2018. Bryophyte biogeography. *Crit. Rev. Pl. Sci.* 37: 175–209. <https://doi.org/10.1080/07352689.2018.1482444>
- Patiño, J., Medina, R., Vanderpoorten, A., González-Mancebo, J.M., Werner, O., Devos, N., Mateo, R.G., Lara, F. & Ros, R.M. 2013.

- Origin and fate of the single-island endemic moss *Orthotrichum handiense*. *J. Biogeogr.* 40: 857–868. <https://doi.org/10.1111/jbi.12051>
- Patiño, J., Carine, M., Mardulyn, P., Devos, N., Mateo, R.G., González-Mancebo, J.M., Shaw, A.J. & Vanderpoorten, A.** 2015. Approximate Bayesian computation reveals the crucial role of oceanic islands for the assembly of continental biodiversity. *Syst. Biol.* 64: 579–589. <https://doi.org/10.1093/sysbio/syv013>
- Patiño, J., Goffinet, B., Sim-Sim, M. & Vanderpoorten, A.** 2016. Is the sword moss (*Bryoxiphium*) a preglacial Tertiary relict? *Molec. Phylogen. Evol.* 96: 200–206. <https://doi.org/10.1016/j.ympev.2015.12.004>
- Patiño, J., Hedenäs, L., Dirkse, G.M., Ignatov, M.S., Papp, B., Müller, F., González-Mancebo, J.M. & Vanderpoorten, A.** 2017. Species delimitation in the recalcitrant moss genus *Rhynchostegiella* (Brachytheciaceae). *Taxon* 66: 293–308. <https://doi.org/10.12705/662.1>
- Pedersen, N., Cox, C.J. & Hedenäs, L.** 2003. Phylogeny of the Moss family Bryaceae inferred from chloroplast DNA sequences and morphology. *Syst. Bot.* 28: 471–482. <https://doi.org/10.1043/02-46.1>
- Pons, J., Barraclough, T.G., Gomez-Zurita, J., Cardoso, A., Duran, D.P., Hazell, S., Kamoun, S., Sumlin, W.D. & Vogler, A.P.** 2006. Sequence-based species delimitation for the DNA taxonomy of undescribed insects. *Syst. Biol.* 55: 595–609. <https://doi.org/10.1080/10635150600852011>
- Preston, C.D. & Hill, M.O.** 1999. The geographical relationships of the British and Irish flora: A comparison of pteridophytes, flowering plants, liverworts and mosses. *J. Biogeogr.* 26: 629–642. <https://doi.org/10.1046/j.1365-2699.1999.00314.x>
- R Core Team** 2019. R: A language and environment for statistical computing. Vienna, Austria.
- Rambaut, A.** 2016. FigTree, version 1.4.3. <http://tree.bio.ed.ac.uk/software/figtree/> (accessed 19 Jul 2018).
- Rambaut, A., Drummond, A.J., Xie, D., Baele, G. & Suchard, M.A.** 2018. Posterior summarisation in Bayesian phylogenetics using Tracer 1.7. *Syst. Biol.* 67: 901–904. <https://doi.org/10.1093/sysbio/syy032>
- Ree, R.H. & Sanmartín, I.** 2018. Conceptual and statistical problems with the DEC+J model of founder-event speciation and its comparison with DEC via model selection. *J. Biogeogr.* 45: 741–749. <https://doi.org/10.1111/jbi.13173>
- Reid, N.M. & Carstens, B.C.** 2012. Phylogenetic estimation error can decrease the accuracy of species delimitation: A Bayesian implementation of the general mixed Yule-coalescent model. *B. M. C. Evol. Biol.* 12: 196. <https://doi.org/10.1186/1471-2148-12-196>
- Renner, M.A.M., Brown, E.A. & Wardle, G.M.** 2010. The *Lejeunea tumida* species group (Lejeuneaceae: Jungermanniopsida) in New Zealand. *Austral. Syst. Bot.* 23: 443. <https://doi.org/10.1071/SB10037>
- Renner, M.A.M., Heslewood, M.M., Patzak, S.D.F., Schäfer-Verwimp, A. & Heinrichs, J.** 2017. By how much do we underestimate species diversity of liverworts using morphological evidence? An example from Australasian *Plagiochila* (Plagiochilaceae: Jungermanniopsida). *Molec. Phylogen. Evol.* 107: 576–593. <https://doi.org/10.1016/j.ympev.2016.12.018>
- Robinson, H.** 1968. Notes on Bryophytes from the Himalayas and Assam. *Bryologist* 71: 82–97. <https://doi.org/10.2307/3240667>
- Ronquist, F., Huelsenbeck, J. & Teslenko, M.** 2011. MrBayes Version 3.2 Manual: Tutorials and Model Summaries. http://mrbaes.sourceforge.net/wiki/index.php/Tutorial_3.2
- Shaw, A.J.** 1984. Quantitative taxonomic study of morphology in *Epipterygium*. *Bryologist* 87: 132–142. <https://doi.org/10.2307/3243119>
- Shaw, A.J.** 2000. Molecular phylogeography and cryptic speciation in the mosses, *Mielichhoferia elongata* and *M. mielichhoferiana* (Bryaceae). *Molec. Ecol.* 9: 595–608. <https://doi.org/10.1046/j.1365-294X.2000.00907.x>
- Shaw, A.J.** 2001. Biogeographic patterns and cryptic speciation in bryophytes. *J. Biogeogr.* 28: 161–253. <https://doi.org/10.1046/j.1365-2699.2001.00530.x>
- Shaw, A.J., Werner, O. & Ros, R.M.** 2003. Intercontinental mediterranean disjunct mosses: Morphological and molecular patterns. *Amer. J. Bot.* 90: 540–550. <https://doi.org/10.3732/ajb.90.4.540>
- Shaw, A.J., Golinski, G.K., Clark, E.G., Shaw, B., Stenøien, H.K. & Flatberg, K.I.** 2014. Intercontinental genetic structure in the amphipacific peatmoss *Sphagnum miyabeanum* (Bryophyta: Sphagnaceae). *Biol. J. Linn. Soc.* 111: 17–37. <https://doi.org/10.1111/bij.12200>
- Simmons, M.P. & Ochoterena, H.** 2000. Gaps as characters in sequence-based phylogenetic analyses. *Syst. Biol.* 49: 369–381.
- Suchard, M.A., Lemey, P., Baele, G., Ayres, D.L., Drummond, A.J. & Rambaut, A.** 2018. Bayesian phylogenetic and phylodynamic data integration using BEAST 1.10. *Virus Evol.* 4(1): vey016. <https://doi.org/10.1093/ve/vey016>
- Sukkharak, P., Gradstein, S.R. & Stech, M.** 2011. Phylogeny, taxon circumscriptions, and character evolution in the core Ptychanthoideae (Lejeuneaceae, Marchantiophyta). *Taxon* 60: 1607–1622. <https://doi.org/10.1002/tax.606006>
- Sukumaran, J. & Holder, M.T.** 2010. DendroPy: A Python library for phylogenetic computing. *Bioinformatics* 26: 1569–1571. <https://doi.org/10.1093/bioinformatics/btq228>
- Tiffney, B.H.** 2000. Geographic and climatic influences on the Cretaceous and Tertiary history of Euramerican floristic similarity. *Acta Univ. Carol., Geol.* 44: 5–16.
- Tiffney, B.H. & Manchester, S.R.** 2001. The use of geological and paleontological evidence in evaluating plant phylogeographic hypotheses in the Northern Hemisphere Tertiary. *Int. J. Pl. Sci.* 162: 3–17. <https://doi.org/10.1086/323880>
- Van der Wijk, R.W., Margadant, D. & Florschütz, P.A.** 1962. *Index Muscorum*, vol. 2 (D–Hypno). Regnum Vegetabile 26. Utrecht: International Bureau for Plant Taxonomy and Nomenclature of the International Association for Plant Taxonomy.
- Vanderpoorten, A. & Shaw, A.J.** 2014. The application of molecular data to the phylogenetic delimitation of species in bryophytes: A note of caution. *Phytotaxa* 9: 229–237. <https://doi.org/10.11646/phytotaxa.9.1.12>
- Vanderpoorten, A., Patiño, J., Désamoré, A., Laenen, B., Gorski, P., Papp, B., Hala, E., Korpelainen, H. & Hardy, O.J.** 2019. To what extent are bryophytes efficient dispersers? *J. Ecol.* 107: 2149–2154. <https://doi.org/10.1111/1365-2745.13161>
- Vigalondo, B., Lara, F., Draper, I., Valcarcel, V., Garilleti, R. & Mazimpaka, V.** 2016. Is it really you, *Orthotrichum acuminatum*? Ascertaining a new case of intercontinental disjunction in mosses. *Bot. J. Linn. Soc.* 180: 30–49. <https://doi.org/10.1111/boj.12360>
- Vigalondo, B., Garilleti, R., Vanderpoorten, A., Patiño, J., Draper, I., Calleja, J.A., Mazimpaka, V. & Lara, F.** 2019a. Do mosses really exhibit so large distribution ranges? Insights from the integrative taxonomic study of the *Lewinskya affinis* complex (Orthotrichaceae, Bryopsida). *Molec. Phylogen. Evol.* 140: 106598. <https://doi.org/10.1016/j.ympev.2019.106598>
- Vigalondo, B., Patiño, J., Draper, I., Mazimpaka, V., Shevock, J.R., Losada-Lima, A., González-Mancebo, J.M., Garilleti, R. & Lara, F.** 2019b. The long journey of *Orthotrichum shevockii* (Orthotrichaceae, Bryopsida): From California to Macaronesia. *PLoS ONE* 14: e0211017. <https://doi.org/10.1371/journal.pone.0211017>
- Villarreal, J.C. & Renner, S.S.** 2014. A review of molecular-clock calibrations and substitution rates in liverworts, mosses, and hornworts, and a timeframe for a taxonomically cleaned-up genus *Nothoceros*. *Molec. Phylogen. Evol.* 78: 25–35. <https://doi.org/10.1016/j.ympev.2014.04.014>
- Wen, J. & Ickert-Bond, S.M.** 2009. Evolution of the Madrean-Tethyan disjunctions and the North and South American amphitropical disjunctions in plants. *J. Syst. Evol.* 47: 331–348. <https://doi.org/10.1111/j.1759-6831.2009.00054.x>

Werner, O., Ros, R.M., Guerra, J. & Shaw, A.J. 2003. Molecular data confirm the presence of *Anacolia menziesii* (Bartramiaceae, Musci) in southern Europe and its separation from *Anacolia web-bii*. *Syst. Bot.* 28: 483–489. <https://doi.org/10.1043/02-42.1>

Werner, O., Ros, R.M. & Grundmann, M. 2005. Molecular phylogeny of Trichostomoideae (Pottiaceae, Bryophyta) based on nrITS sequence data. *Taxon* 54: 361–368. <https://doi.org/10.2307/25065364>

Wiens, J.J. & Graham, C.H. 2005. Niche conservatism: Integrating evolution, ecology, and conservation biology. *Annual Rev. Ecol. Evol. Syst.* 36: 519–539. <https://doi.org/10.1146/annurev.ecolsys.36.102803.095431>

Zhang, J., Kapli, P., Pavlidis, P. & Stamatakis, A. 2013. A general species delimitation method with applications to phylogenetic placements. *Bioinformatics* 29: 2869–2876. <https://doi.org/10.1093/bioinformatics/btt499>

Appendix 1. Descriptive statistics for quantitative characters of *Epipterygium tozeri* of different geographical origin (mean \pm SD [range]) including ANOVA F statistic and significance level (* $P \leq 0.05$, ** $P \leq 0.005$, *** $P < 0.001$). Letters in parentheses (a, b, c, d) represent results from a post-hoc Tukey test for statistically significant variables.

	Continental	Macaronesia	Asia	U.S.A.	Yunnan	Japan	ANOVA
Analyzed collections	<i>T. Arts 339141-29</i> (BR), <i>T. Arts 339149-37</i> (BR)	<i>A. Vanderpoorten 070312</i> (LG), <i>T. Arts 339139-27</i> (BR)	<i>D.G. Long s.n.</i> (E00884194), <i>D.G. Long s.n.</i> (E0084196)	<i>J. Brinda 5770</i> (MO), <i>J. Brinda 3131</i> (MO)	<i>D.G. Long s.n.</i> (E00576940)	<i>Z. Iwatsuki 160338</i> (NICH), <i>Z. Iwatsuki 172095</i> (NICH)	
Stem length [mm]	8.71 \pm 2.01 [6.2–13] (a)	2.99 \pm 0.49 [2.4–3.9] (c)	3.57 \pm 0.46 [3–4.4] (c)	6.39 \pm 0.80 [5.3–7.4] (b)	8.42 \pm 0.91 [7–9.1] (ab)	7.61 \pm 1.91 [5.2–10] (ab)	1.38e-14***
Costa length [mm]	1.59 \pm 0.32 [1.07–2.02] (a)	0.81 \pm 0.25 [0.25–1.07] (c)	0.8 \pm 0.13 [0.62–1.07] (c)	1.68 \pm 0.36 [1.12–2.35] (a)	1.13 \pm 0.12 [1.05–1.35] (bc)	1.51 \pm 0.19 [1.17–1.77] (ab)	6.76e-12***
Lateral leaf length [mm]	2.15 \pm 0.31 [1.62–2.55] (ab)	1.8 \pm 0.20 [1.5–2.12] (b)	1.31 \pm 0.14 [1.05–1.52] (c)	2.20 \pm 0.36 [1.6–2.72] (a)	1.77 \pm 0.22 [1.62–2.12] (bc)	2.00 \pm 0.32 [1.37–2.5] (ab)	2.58e-08***
Lateral leaf width [mm]	0.99 \pm 0.18 [0.77–1.27] (a)	0.95 \pm 0.11 [0.85–1.22] (a)	0.74 \pm 0.13 [0.6–1] (b)	0.81 \pm 0.18 [0.57–1.15] (ab)	0.93 \pm 0.07 [0.85–1.02] (ab)	0.86 \pm 0.13 [0.62–1] (ab)	0.00181**
Lateral leaf length/width	2.20 \pm 0.30 [1.83–2.80] (bc)	1.82 \pm 0.24 [1.45–2.42] (cd)	1.79 \pm 0.22 [1.5–2.16] (d)	2.77 \pm 0.50 [2.36–4] (a)	1.88 \pm 0.12 [1.71–2.07] (bcd)	2.33 \pm 0.14 [2.14–2.5] (b)	3.97e-09***
Dorsal leaf length [mm]	1.23 \pm 0.17 [1–1.42] (a)	0.87 \pm 0.15 [0.65–1.02] (c)	0.94 \pm 0.15 [0.75–1.17] (bc)	1.22 \pm 0.34 [0.75–1.6] (ab)	0.83 \pm 0.21 [0.62–1.1] (c)	0.97 \pm 0.19 [0.75–1.25] (abc)	0.000278***
Dorsal leaf width [mm]	0.43 \pm 0.073 [0.35–0.6] (ab)	0.34 \pm 0.16 [0.12–0.5] (b)	0.49 \pm 0.09 [0.37–0.62] (a)	0.32 \pm 0.07 [0.225–0.425] (b)	0.46 \pm 0.17 [0.3–0.7] (ab)	0.43 \pm 0.08 [0.35–0.6] (ab)	0.0086**
Dorsal leaf length/width	2.90 \pm 0.43 [2.33–3.8] (abc)	3.20 \pm 1.74 [2.05–6.4] (ab)	1.93 \pm 0.24 [1.76–2.4] (c)	3.76 \pm 0.56 [3–4.26] (a)	1.84 \pm 0.23 [1.57–2.08] (c)	2.25 \pm 0.24 [1.68–2.5] (bc)	2.51e-05***
Median cell length [μ m]	170 \pm 30.68 [125–222.5] (a)	127.25 \pm 21.87 [90–150] (b)	79.75 \pm 19.38 [62.5–110] (c)	112.25 \pm 17.96 [85–137.5] (b)	120 \pm 6.84 [112.5–125] (b)	112.5 \pm 8.57 [100–127.5] (b)	3.44e-11***
Median cell width [μ m]	34.5 \pm 6.10 [25–45] (a)	28.25 \pm 3.12 [22.5–32.5] (bc)	24 \pm 6.47 [15–37.5] (c)	24.5 \pm 2.58 [20–30] (bc)	31.5 \pm 4.54 [27.5–37.5] (ab)	25.25 \pm 0.79 [25–27.5] (bc)	6.29e-06***
Median cell length/width	5.01 \pm 1.05 [3.33–7.41] (a)	4.48 \pm 0.42 [3.81–5] (ab)	3.37 \pm 0.47 [2.7–4.16] (c)	4.60 \pm 0.74 [3.6–6.11] (ab)	3.87 \pm 0.57 [3.21–4.54] (bc)	4.45 \pm 0.29 [4–5.1] (ab)	2.38e-05***
Marginal cell length [μ m]	210.25 \pm 15.74 [187.5–237.5] (a)	189 \pm 34.07 [135–237.5] (a)	142 \pm 22.41 [115–187.5] (b)	183 \pm 30.06 [125–232.5] (a)	175.5 \pm 14.29 [152.5–187.5] (ab)	147.75 \pm 17.13 [125–175] (b)	2.68e-07***
Marginal cell width [μ m]	11.25 \pm 1.76 [7.5–12.5] (a)	10.75 \pm 1.20 [10–12.5] (a)	8.25 \pm 1.20 [7.5–10] (b)	8.5 \pm 1.29 [7.5–10] (b)	8 \pm 1.11 [7.5–10] (b)	9.5 \pm 1.97 [7.5–12.5] (ab)	2.91e-05***
Marginal cell length/width	18.83 \pm 4.18 [16–29.66] (ab)	17.52 \pm 2.04 [13.5–20.25] (ab)	17.31 \pm 2.28 [13.75–21] (ab)	22.05 \pm 5.22 [12.5–31] (a)	22.23 \pm 3.26 [17.5–25] (a)	15.93 \pm 2.56 [12.75–20.33] (b)	0.00133**

Appendix 2. Accession list with geographic origin, voucher information, GenBank accession numbers (*ITS*, *trnG*, *trnT-psbD*). Sequences downloaded from GenBank indicated with an asterisk.

Epipterygium atlanticum Hanusch sp. nov. — PORTUGAL: Azores, Pico, *A. Vanderpoorten 020312* (LG) MK622501, MK622599, MK622685; Azores, São Jorge, *A. Vanderpoorten 060312* (LG) MK622504, MK622620, MK622688; Azores, São Jorge, *A. Vanderpoorten 070312* (LG) MK622505, MK622603, MK622689; Azores, São Jorge, *A. Vanderpoorten 040312a* (LG) MK622503, MK622601, MK62268; Azores, São Jorge, *A. Vanderpoorten 040312b* (LG) MK622502, MK622600, MK622686; Azores, São Miguel, *A. Schäfer-Verwimp 29625* (TUM) MK622440, MK622541, MK622641; Azores, São Miguel, *J. Patiño 108JP* (LG) MK622485, MK622581, MK622669; Azores, São Miguel, *J. Patiño 104JP* (LG) MK622477, MK622574, –; Azores, Faial, *A. Vanderpoorten 080312* (LG) MK622506, MK622604, MK622690; Azores, Terceira, *A. Schäfer-Verwimp 33545* (TUM) MK622441, MK622542, MK622642; Madeira, Funchal, *A. Hübschmann 0289797* (M) MK622454, –, –; Madeira, Rocha Negra, *L. Hedenäs B22496* (S) MK622480, MK622677; Madeira, Curral das Freiras, *T. Arts 339139-27* (BR) –, MK622583, MK622671; Madeira, Ribeiro Frio, *T. Arts 170388* (BR) –, MK622585, MK622672; Madeira, Ribeira Brava, *R. Düll 0289798* (M) MK622455, MK622554, –; Madeira, Porto Moniz, *G.M. Dirkse 28594* (LG) MK622512, MK622610, MK622696. SPAIN: Canary Islands, Gran Canaria, *M. Hanusch CI012* (TUM) MK622423, MK622523, MK622624; Canary Islands, Gran Canaria, *M. Hanusch CI013* (TUM) MK622424, MK622524, MK622625; Canary Islands, La Gomera, *R. Hernández 250112* (LG) MK622493, MK622591, MK622677; Canary Islands, La Gomera, *G.M. Dirkse 23670* (LG) MK622511, MK62260, MK622695; Canary Islands, La Gomera, *R. Hernández 150112* (LG) MK622492, MK622590, MK622676; Canary Islands, La Gomera, *J. Patiño 76JP* (LG) MK622475, MK622572, MK622663; Canary Islands, La Palma, *M. Hanusch CI005* (TUM) MK622416, MK622517, MK622619; Canary Islands, La Palma, *M. Hanusch CI006* (TUM) MK622417, –, –; Canary Islands, La Palma, *M. Hanusch CI007* (TUM) MK622418, MK622518, MK622620; Canary Islands, La Palma, *M. Hanusch CI008* (TUM) MK622419, MK622519, –; Canary Islands, La Palma, *M. Hanusch CI009* (TUM) MK622420, MK622520, MK622621; Canary Islands, La Palma, *M. Hanusch CI010* (TUM) MK622421, MK622521, MK622622; Canary Islands, La Palma, *M. Hanusch CI011* (TUM) MK622422, MK622522, MK622623; Canary Islands, La Palma, *A. Vanderpoorten LP30* (LG) MK622494, MK622592, MK622678; Canary Islands, La Palma, *A. Vanderpoorten LP81* (LG) MK622495, MK622593, MK622679; Canary Islands, La Palma, *A. Vanderpoorten LP53* (LG) MK622500, MK622598, MK622684; Canary Islands, La Palma, *A. Vanderpoorten LP11* (LG) MK622499, MK622597, MK622683; Tenerife, *T. Arts 24227* (BR) MK622614, –, MK622700; Canary Islands, Tenerife, *A. Vanderpoorten TEN10* (LG) MK622497, MK622595, MK622681; Canary Islands, Tenerife, *A. Vanderpoorten TEN7* (LG) MK622498, MK622596, MK622682; Canary Islands, Tenerife, *T. Arts 24059* (BR) MK622487, MK622584, –; Canary Islands, Tenerife, *M. Hanusch CI001* (TUM) MK622414, MK622515, MK622617; Canary Islands, Tenerife, *M. Hanusch CI002* (TUM) MK622415, MK622516, MK622618; Canary Islands, Tenerife, *G.M. Dirkse 23696* (LG) MK622510, MK622608, MK622694; UNITED KINGDOM: Scotland, Aberdeen, *Lawley 2004BBSUK* (LG) MK622509, MK622607, MK622693. *Epipterygium bairiumum* Hanusch sp. nov. — UNITED STATES: California, *J. Brinda 5770* (MO) MK622428, MK622528, MK622628; California, *J. Brinda 5726* (MO) MK622430, MK622531, MK622631; Washington, *J. Brinda 10937* (MO) –, MK622529, MK622629; California, *J. Brinda 5776* (MO) MK622431, MK622532, MK622632; Oregon, *J. Brinda 3131* (MO) MK622429, MK622530, MK622630; California, *R. Düll 0289801* (M) MK622456, MK622555, –. *Epipterygium convalleum* Dusen — EQUATORIAL GUINEA: Bioko, *F. Mueller 047380* (DR) MK622438, MK622539, MK622639; UGANDA: Rukungiri, Bwindi Impenetrable Forest, *M.J. Wigginton 5091b* (DR) LC542980, LC542979, –. *Epipterygium immarginatum* Mitt. — BOLIVIA: La Paz, *A. Fuentes 11173* (MO) MK622463, MK622560, MK622656; COSTA RICA: San Jose, *A. Schäfer-Verwimp 0224* (TUM) MK622449, MK622549, MK622650; San Jose, *A. Schäfer-Verwimp 0269* (TUM) MK622451, MK622551, MK622652; ECUADOR: Zamora-Chinchipe, *S. Churchill 24118* (MO) MK622464, MK622561, MK622657; Zamora-Chinchipe, *A. Schäfer-Verwimp 23413* (TUM) MK622448, –, MK622649; Pinchincha, *A. Schäfer-Verwimp 24137* (TUM) MK622433, MK622550, MK622651. *Epipterygium mexicanum* (Besch.) Broth. — COSTA RICA: Talamanca, *A. Schäfer-Verwimp CR-99-1169B* (NY) MK622432, MK622533, MK622633; Talamanca, *A. Schäfer-Verwimp 0078* (TUM) MK622452, MK622552, –; Honduras, Lempira, *B. Allen 11158* (MO) MK622466, MK622563, MK622659; Talamanca, *I. Holz CR99-0467* (MO) MK622467, MK622564, MK622660; EL SALVADOR: San Salvador, *A. Monro 2262* (MO) MK622616, –, –; MEXICO: Mpio, *W. Buck 28150* (NY) MK622434, MK622535, MK622635; Tepoztlán, *C. Delgadillo 5638* (NY) MK622450, MK622534, MK622634; Veracruz, *W. Buck 35361* (NY) MK622435, MK622536, MK622636. *Epipterygium orbifolium* (Müll.Hal.) Müll.Hal. — UNITED STATES: Puerto Rico, El Yunque, *M.J. Price 960* (MO) MK622457, MK622556, –; Puerto Rico, Rio Grande, *I. Sastre 1701* (MO) MK622458, –, –; DOMINICA: Roseau Valley, *A. Schäfer-Verwimp 17617* (TUM) MK622444, MK622545, MK622645; DOMINICAN REPUBLIC: La Vega, *W. Buck 636313* (NY) MK622437, MK622538, MK622638. *Epipterygium oreophilum* Hanusch sp. nov. — BHUTAN: Tongsa, *D.G. Long s.n.* (E barcode E00884194) MK622473, MK622570, MK622661; NEPAL: Sankhuwasabha, *D.G. Long s.n.* (E barcode E00576939) MK622472, MK622569, –; Dobala Danda, *D.G. Long s.n.* (E barcode E00576938) MK622471, MK622568, –; Rasuma, *D.G. Long s.n.* (E barcode E00576937) MK622470, MK622567, –; P.R. CHINA: Yunnan, *D.G. Long s.n.* (E barcode E00576941) MK622468, MK622565, –. *Epipterygium puiggarii* (Geh. & Hampe) Broth. — BOLIVIA: Tarija Arce, *S. Churchill 23266-A* (MO) MK622460, MK622558, MK622654; Belisario Boeto, *S. Churchill 22960* (MO) MK622461, –, –; Tarija Arce, *H. Huyalla 1744* (MO) MK622462, MK622559, MK622655; Padacaya, *S. Churchill 23601-A* (MO) MK622459, MK622557, –; BRAZIL: Parana, *A. Schäfer-Verwimp 15176* (TUM) MK622442, MK622543, MK622643; Parana, *A. Schäfer-Verwimp 15119* (TUM) MK622453, MK622553, MK622653; Rio de Janeiro, *A. Schäfer-Verwimp 13098a* (TUM) MK622443, MK622544, MK622644; Minas Gerais, *W. Buck 2082071* (NY) MK622436, MK622537, MK622637. *Epipterygium tozeri* (Grev.) Lind. — FRANCE: Roquebrune, *A. Vanderpoorten 190210* (LG) MK622514, MK622613, MK622699; Maures, *A. Vanderpoorten ONF113* (LG) MK622513, MK622612, MK622698; Corse, *A. Vanderpoorten COR2207165* (LG) –, MK622611, MK622697; GREECE: Chalkidiki, *F. Müller 047355* (DR) MK622427, MK622527, MK622627; IRAN: Mazandaran, *H. Zarre B173486* (S) MK622496, MK622594, MK622680; IRELAND: Cork, *Bosanquet BBSUK2009* (LG) MK622507, MK622605, MK622691; Waterford, *Holyoak 2007BBSUK* (LG) MK622508, MK622606, MK622692; ITALY: Sardinia, *F. Müller 047379* (DR) MK622426, MK622526, MK622626; Sicily, *F. Müller 047378* (DR) MK622425, MK622525, –; PORTUGAL: Algarve, *T. Arts 339146-47* (BR) –, MK622615, –; Algarve, *T. Arts 19820* (BR) MK622489, MK622587, MK622673; Algarve, *T. Arts 339149-37* (BR) MK622483, MK622579, MK622667; Algarve, *A. Schäfer-Verwimp 17490* (TUM) MK622439, MK622540, MK622640; Douro Litoral, *C. Garcia 239533* (LG) MK622476, MK622573, MK622664; Minho, *C. Garcia 239533* (LISU) MK622490, MK622588, MK622674; Alto Douro, *C. Sérgio 239537* (LISU) MK622484, MK622580, MK622668; Madeira, Santo da Serra, *T. Arts 339141-29* (BR) MK622486, MK622582, MK622670; SPAIN: Algeciras, *N. Hakeliet 43788* (S) MK622481, MK622578, MK622666; Algeciras, *J. Leal 106JP* (LG) MK622479, MK622576, MK622665; Algeciras, *J. Leal 105JP* (LG) MK622478, MK622575, –; Granada, *T. Arts 20420* (BR) MK622488, MK622586, –; Huelva, *R.M. Cros 55335* (BCB) MK622491, MK622589, MK622675; Málaga, *N. Hakeliet 43787* (S) MK622482, –, –. *Epipterygium wrightii* (Sull.) Lindb. — JAMAICA: St. James, *A. Schäfer-Verwimp 35027* (TUM) MK622445, MK622546, MK622646; Portland, *A. Schäfer-Verwimp 35272* (TUM) MK622446, MK622547, MK622647; Portland, *A. Schäfer-Verwimp 34935* (TUM) MK622447, MK622548, MK622648; HONDURAS: Comayagua, *B. Allen 11786* (MO) MK622465, MK622562, MK622658. *Epipterygium yunnanense* Hanusch sp. nov. — P.R. CHINA: Yunnan, *D.G. Long s.n.* (E barcode E00576940) MK622469, MK622566, –. *Pohlia elongata* Hedw. — FJ796886.1*, –, KX289675.1*.

Appendix 3. Model comparison of Yule model, Birth-Death model and Coalescent model with constant population size according to path sampling and stepping-stone analysis under a strict clock and an uncorrelated lognormal relaxed clock.

	Path sampling		Stepping-stone	
	ln (MLE)	2ln (BF)	ln (MLE)	2ln (BF)
ST-YL	-7848.01	495.54	-7848.42	495.55
ST-BD	-7770.41	340.34	-7770.58	339.87
ST-CS	-7785.82	371.15	-7786.66	372.02
UCLD-YL	-7646.16	91.83	-7648.66	96.03
UCLD-BD	-7600.24	0	-7600.64	0
UCLD-CS	-7612.17	23.858	-7613.66	26.036

ST, strict clock; UCLD, uncorrelated lognormal relaxed clock; YL, Yule model; BD, birth-death model; CS, coalescent model with constant population size. Marginal likelihood estimates (MLE), the difference between the models and the most likely model, as well as resulting Bayes factors (BF) are given. The best model is highlighted in bold.

Appendix 4. Performance of competing models of ancestral range estimation in the moss genus *Epipterygium*.

	LnL	<i>n</i>	<i>d</i>	<i>e</i>	AIC	AICc	w-AICc	ΔAICc
DEC	-49.66	2	0.018	1e-12	103.4	105.8	0.032	6.1
DIVALIKE	-46.94	2	0.022	1e-12	98.0	99.7	0.47	0
BAYAREALIKE	-90.30	2	0.010	0.089	184.7	152.6	6.914e-20	52.9

lnL, log-likelihood; *n*, number of parameters; *d*, rate of dispersal; *e*, rate of extinction; AIC, Akaike information criterion; AICc, Akaike information criterion corrected for small sample sizes; w-AICc, Akaike weight; ΔAICc, AICc difference; DEC, dispersal-extinction-cladogenesis; DIVA, dispersal-vicariance analysis. The best model is highlighted in bold.